Ofioliti, 2026, 51 (2), 107-133 - doi: 10.4454/ofioliti.v51i2.584

A REVIEW OF MELT, FLUID AND SOLID-PHASE TRANSFERS IN THE NEW CALEDONIA FOREARC OPHIOLITE

Dominique Cluzel*,✉, Marc Ulrich*,, Pengjie Cai***, Jonathan C. Aitchison•, Claudio Marchesi••,•••, Pierre Maurizot°, Alessandra Montanini°°** and **Arianna Secchiari°°°**

* *Institut de Sciences Exactes et Appliquées, Université de la Nouvelle Calédonie, New Caledonia.*
** *Institut Terre et Environnement de Strasbourg-EOST, CNRS-UMR 7063, Université de Strasbourg, France.*
*** *IMM, State Key Laboratory for Mineral Deposits Research, School of Earth Sciences and Engineering, Nanjing University, China.*
• *School of the Environment, University of Queensland, St Lucia, Australia.*
•• *Departamento de Mineralogía y Petrología, Universidad de Granada, Spain.*
••• *Materias Primas, Salud Humana y Ambiental, UGR, Unidad Asociada al CSIC por el IACT-CSIC, Armilla, Granada, Spain.*
° *Geological Survey of New Caledonia, Nouméa, New Caledonia.*
°° *Dipartimento di Scienze Chimiche, della Vita e della Sostenibilità Ambientale, Università di Parma, Italy.*
°°° *Department of Earth Sciences "A. Desio" University of Milan, Milano, Italy.*
✉ *Corresponding author, e-mail: dominique.cluzel@unc.nc*

Keywords: *New Caledonia; ophiolite; forearc, transfer; fluids; magma; solid; mantle metasomatism.*

ABSTRACT

The Eocene Peridotite Nappe of New Caledonia is a natural laboratory for forearc ophiolite processes and their impact on mantle rocks. The ophiolite includes highly refractory harzburgite-dunite association (up to 2500 m thick) with minor lherzolites, overlain by mafic and ultramafic cumulates forming a proto-arc lower crust. The mafic-ultramafic association was obducted during the latest stages of Eocene subduction (~34 Ma). Harzburgites, which constitute most of the ophiolite, are highly residual and preserve evidence for hydrous melting superimposed on an earlier anhydrous melting event. Their broad isotopic variability further reflects the evolution of an ultra-depleted fore-arc mantle, variably overprinted by fluid and melt inputs during Eocene subduction. Combined mineralogical, geochemical, and Sr-Nd-Pb isotope data indicate melting accompanied by syn- to post-melting metasomatism driven by slab-derived fluids and melts. Lherzolites, restricted to the northern massifs, may represent the remnants of a pre-Eocene marginal basin located to the east of New Caledonia/Norfolk Ridge. These moderately depleted rocks show evidence for anhydrous melting and post-melting re-enrichment. The ophiolite is crosscut by a diverse suite of pre-obduction dikes (55-50 Ma), generated mainly from adakitic slab melts that variably interacted with mantle-wedge peridotites, producing secondary melts, which differentiated into boninite-series felsic dikes and rare clinoenstatite boninites. Boninite-like and highly depleted tholeiitic melts interacted with harzburgites, producing a thick dunite transition zone and associated cumulate lenses composed of wehrlites, websterites, and gabbronorites.

The occurrence of diverse xenocrysts (rutile, zircon, low $\delta^{13}C$ diamond and moissanite) in unserpentinized peridotites and chromite pods documents fluid-driven solid-phase transfer from subducted sediments into the mantle wedge peridotites.

At lower temperatures, slab-derived hydrous fluids circulation led to the serpentinization of the mantle wedge peridotites, up to 100% near the base of the ophiolite. The fractures in already serpentinized peridotites were locally infiltrated by Ca(-Sr)-rich hydrous fluids derived from the leaching of felsic dikes and reactivated in a transcurrent regime. Syntectonic Ca metasomatism resulted in tremolite formation, then antigorite+tremolite and finally antigorite-bearing crack seals with the exhaustion of Ca-rich fluids. At the end of the episode of forearc magmatism (50-47 Ma), island-arc tholeiitic dikes associated with slab steepening and mantle upwelling intruded the already cooled forearc peridotites. Subsequent evolution relates to post-obduction supergene evolution (33 Ma-present), while serpentinization in deep parts of the ophiolite is still moderately active and marked by hydrogen seepage in hyperalkaline springs.

Overall, the New Caledonia ophiolite records a polyphase evolution of the forearc mantle, documenting successive melting events and pervasive metasomatic overprint driven by fluid, melt and solid phase transfers from the slab to the mantle wedge and within the mantle wedge itself.

INTRODUCTION

Since the early definition by Alexandre Brongniart (1813), ophiolites (etymologically "snake rock" due to the occurrence of serpentine thought to cure snake bites in ancient times) have been a continuous object of attention and debate. In its modern sense, the concept of ophiolite covers all rock assemblages that originated from the oceanic lithosphere and were tectonically emplaced on a continental margin (e.g. Moores, 1982; Shervais, 2001; Dilek, 2003). An ophiolite may be emplaced either from downgoing oceanic lithosphere via subduction-accretion (Cordilleran type) or from the upper plate in a subduction zone through trench-continent collision (Tethyan type) (Beccaluva et al., 2004; Dilek and Furnes, 2014). Ophiolites derived from the lower plate by subduction accretion are generally tectonically sliced at low or moderate temperature, thus strongly deformed and dominated by oceanic crustal material of MORB affinity. In contrast, Tethyan or supra-subduction zone (SSZ) ophiolites display more complete and continuous ultramafic-mafic sequences, which have been strongly affected by various processes due to transfers from the downgoing plate into the mantle wedge. SSZ ophiolites have the geochemical characteristics of island arcs but the structure of oceanic crust and are thought to have formed by seafloor spreading directly above subducted oceanic lithosphere. They differ from 'MORB' ophiolites not only in crust geochemistry but also in the more depleted nature of their mantle sequences and the more common presence of podiform chromite deposits (Pearce et al., 1984). Despite the extreme depletion of SSZ mantle rocks in incompatible elements, modern analytical methods and novel isotopic approaches highlight various processes that reveal the complex evolution of the supra-subduction mantle. Thanks to its rugged topography and man-made outcrops resulting from nickel mining, New Caledonia preserves excellent exposures of ophiolitic rocks. Additionally, the Eocene obduction did not lead to continent-continent collision, so the ophiolite avoided the tectonic dismemberment that occurs in most collisional orogens.

This article presents a comprehensive review of geological, geochemical, and isotopic data published on the New Caledonia Ophiolite over the past three decades, with the aim of synthesizing current understanding of melt-fluid-solid phase transfer processes in a forearc setting. The compiled dataset provides key insights into the complex interplay between melts, aqueous fluids, and mantle peridotites, documenting the pathways and mechanisms of material transfer from the subducting slab to the overlying mantle wedge, as well as the redistribution and interaction of these components within the mantle wedge itself. Particular emphasis is placed on how these processes control metasomatism, element mobility, and the chemical evolution of the forearc lithosphere.

GEOLOGIC SETTING

The New Caledonia archipelago in the south-west Pacific is located within a complex set of marginal basins and continental or volcanic arc ridges. It comprises several islands that form part of the parallel New Caledonia/Norfolk and Loyalty ridges. The main island (known as "Grande Terre") belongs to the New Caledonia/Norfolk Ridge, representing the northern part of the largely submerged Zealandia continent (Luyendyk, 1995; Mortimer et al., 2017) (Fig. 1a). The Belep Islands, located north of the main island, and the Isle of Pines, located south, also belong to the New Caledonia/Norfolk Ridge.

The New Caledonian ophiolite, also known as the Peridotite Nappe (PN), is part of the ultramafic belt, which extends from Papua New Guinea to New Caledonia (Rodgers, 1975) and farther south (Patriat et al., 2018). Peridotite Nappe was first described by Avias (1967) and named by Paris (1981). It consists mainly of ultra-depleted and strongly foliated harzburgites and dunites, a dunitic transition zone and mafic/ultramafic cumulate lenses (in the south). Lherzolites are only present in northern massifs, closely associated with chromitite pods. The Peridotite Nappe covers an area of about 7,000 km²; it extends 540 km from the Belep Islands in the northwest to Pines Island in the southeast (Fig. 1b). Additionally, ultramafic rocks were dredged over c. 1,200 km to the south, establishing a connection with the ophiolites of northern New Zealand (Patriat et al., 2018).

On the main island of New Caledonia (Grande Terre), the Peridotite Nappe comprises a large unit in the southeast (Massif du Sud), which extends along the east coast (c. 4,150 km²). Tectonic klippes (25-350 km²) are spread along the west coast and in the Belep Islands, while a few small units (3-30 km²) are isolated in the island's highlands (Fig. 1b). These klippes are erosional remnants of the large allochthonous unit that initially covered most of the island surface and is interpreted as part of the Loyalty forearc mantle wedge (Aitchison et al., 1995; Cluzel et al., 2001, 2016). The Peridotite Nappe was thrust southwestward over a substrate consisting of sedimentary, volcanic and metamorphic rocks ranging in age from the Permian to the Latest Eocene (Cluzel et al.,

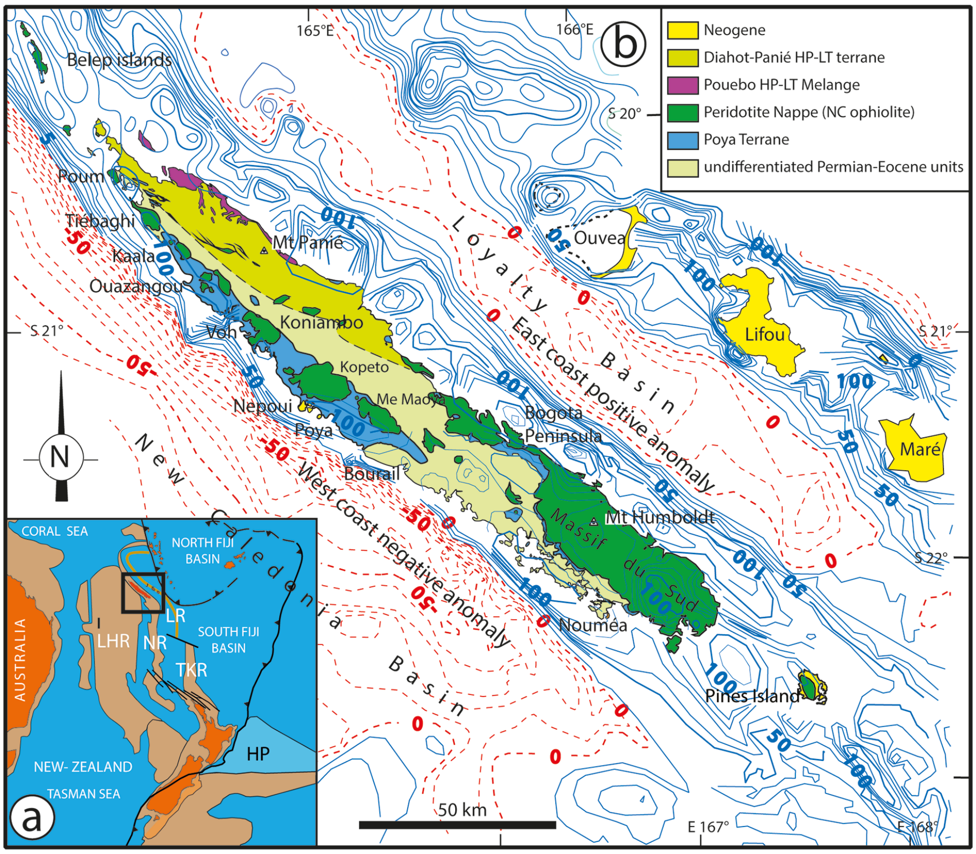

Fig. 1 - (a) Sketch map of the SW Pacific. Red: land; pale red: thinned continental crust areas (submerged); white: oceanic crust areas. LHR: Lord Howe Rise; NR: Norfolk Ridge; LR: Loyalty Ridge; HP: Hikurangi Plateau. (b) Geological map of New Caledonia (redrawn and simplified from the online geological map of New Caledonia (DIMENC-SGNC-BRGM, 2010). The free air anomaly gravity map of New Caledonia and adjacent basins is modified from Collot et al. (1987) and Van de Beuque (1999).

2001; Maurizot et al., 2020a,b). Small, upper Oligocene (c. 24.5 Ma) granodiorite intrusions intersect with the Peridotite Nappe and its substrate, which loosely constrains the timing of ophiolite obduction to the latest Eocene to upper Oligocene period.

The PN is less than 1,000 meters thick in the massifs along the west coast and is probably no more than 2,500 meters thick in the Massif du Sud. The base of the Peridotite Nappe is made up of a porphyroclastic mylonite layer known as the "serpentinite sole". Its variable thickness (20-200 metres) is due to tectonic replication by shallow-dipping thrusts, as well as the accumulation of serpentinite breccia in depressions of the substrate. Except for rare locations (Me Maoya Massif), the degree of serpentinisation decreases from 100% at the base to 60-80%, with only a few nuclei completely escaping serpentinisation (referred to as the "green upper facies" by nickel mining geologists).

High-temperature amphibolite lenses, which are a few hundred meters in length and a few tens of meters thick at most, are pinched beneath the serpentinite and the Peridotite Nappe substrate. Geochemically, they are similar to the back-arc basin basalts of the Poya terrane (see below), and it is thought that they resulted from the HT-LP metamorphism of basalt lenses that had been scraped off beneath the hot overriding lithosphere during the inception of subduction at, or close to, a spreading ridge. Geochronological evidence (U-Pb on zircon overgrowths and $^{40}Ar/^{39}Ar$ on hornblende) yielded a metamorphic recrystallization age of approximately 56 Ma, which is interpreted as marking the timing of subduction inception (Cluzel et al., 2012). The Peridotite Nappe is rooted in the Loyalty Basin, as evidenced by the presence of a narrow positive gravity anomaly (+100 mGal) running parallel to the east coast of Grande Terre (Collot and Missègue, 1986; Collot et al., 1988; Auzende et al., 2000) (Fig. 1b). To the northeast of the root zone, it extends into the gently northeast-dipping basement of the Neogene to Recent Loyalty Basin (Fig. 1b) (Shor et al., 1971; Pontoise et al., 1982; Bitoun and Recy, 1982). The positive gravity anomaly also marks the 300 km extension of the root zone of the ultramafic complex north of the Belep Islands (Collot et al., 1988). The northeast dip of the Moho and the fan-like geometry of the seismic reflectors at the base of the sedimentary strata (Fig. 1S) indicate syn-tilt, i.e. syn-obduction infill (Bitoun and Récy, 1982). In contrast, the upper 80% of the sedimentary strata accumulated horizontally, suggesting post-tilt, i.e. post-obduction sedimentation. Top to the SW emplacement is revealed by kinematic indicators from the serpentinite sole (Gautier et al., 2016; Le Bayon et al., 2023; Maurizot et al., 2023).A variety of dikes displaying supra-subduction geochemical signatures crosscut the ophiolite at all levels, though there is a higher density near the base. These dikes were emplaced during the lower Eocene (55.5-50 Ma, U-Pb zircon and 50-47 Ma, $^{40}Ar/^{39}Ar$ for basalts) shortly after subduction inception (Cluzel et al., 2006, 2024).

Throughout the study area, the Poya Terrane lies beneath the Peridotite Nappe (Fig. 1b). It is subdivided into two units: the Poya Terrane Basalts (PTB) and the Koné Formation (KF). PTB is an allochthonous set of m- to km- thick upright tectonic slices of pillowed and massive basalt associated with thin inliers of bathyal sediments (red, black and green argillite and chert). The main body of this unit is located along the west coast where it is 10 km wide, and extends over a length of 250 km from Bourail to Koumac; smaller and less continuous units are located along the east coast and beneath the front thrust of the Massif du Sud (Fig. 1b). Outcrops of the PTB generate a magnetic anomaly, which extends northwestward over 200 km (up to 18°S) from the northern tip of the island, marking the northern submarine extension of the PTB (Collot et al., 1988).

Paleomagnetic evidence suggest that PTB erupted to form the oceanic floor of the South Loyalty Basin (Cluzel et al., 2001) to the north-east of New Caledonia, about 300 km north of its current location (Ali and Aitchison, 2000). Inliers of bathyal sedimentary rocks, which are closely associated with pillow basalts, contain Campanian-latest Paleocene or earliest Eocene radiolarians (Aitchison et al., 1995b; Cluzel et al., 2001). Poya Terrane basalts are dominantly tholeiitic and represent remnants of an oceanic or marginal basin crust (Cluzel et al., 2001, 2017). Subordinate intra-oceanic alkaline basalts display micritic interpillow material with Late Paleocene-Early Eocene microfaunas. Minor dolerite dikes with E-MORB affinities emplaced later in the early Eocene. Owing to the overall characteristics exposed above, the Poya Terrane basalts may be considered a cordilleran-type ophiolite (Cluzel et al., 2017).

The Koné Formation underlies the PTB tectonically. It consists of Late Cretaceous, fine-grained, passive margin turbidites, intruded by dolerite sills 10 to 100 m thick. Paleontological evidence and zircon provenance data show that the KF is coeval to the autochthonous Formation à Charbon (Cluzel et al., 2017). Large dolerite sills with EMORB affinities were intruded at c. 55 Ma (Lower Eocene, U-Pb zircons) and developed contact metamorphism (Cluzel et al., 2017).

Except for its northernmost exposure along the east coast, where blueschist-facies minerals are scarce and occur with ductile deformation (Meffre, 1995; Cluzel et al., 2017), the Poya Terrane is not regionally metamorphosed and shows no ductile deformation. Only a few localities directly beneath the Peridotite Nappe display a rough schistosity over a few meters below the basal contact. Slices of Poya Terrane rocks were first scraped off the upper part of the crust of the South Loyalty Basin (the lower plate) during NE-dipping subduction (Cluzel et al., 2001). They were then accreted in a forearc region and thrust onto New Caledonia during the Late Eocene, as recorded by clinopyroxene-rich foreland turbidites (Maurizot and Cluzel, 2014; Cluzel et al., 2025). Basalt accretion, underplating and thrusting over the New Caledonia/Norfolk Ridge occurred c. 5-6 Ma prior to the obduction of ultramafic rocks at the end of the Eocene (Cluzel et al., 2025).

Though not strictly demonstrated, it is generally assumed that New Caledonia emerged shortly after obduction in the early Oligocene period. Furthermore, the erosion of regolith material documented in the Lower Miocene Népoui Formation (Coudray, 1976; Sevin et al., 2014; Sevin et al., 2020) suggests that tropical weathering began during the Oligocene. This view is supported by the paleomagnetic dating of the lateritic iron crusts on the Tiebaghi Massif, which date to the Late Oligocene (25 Ma) (Sevin et al., 2012) and probably mark the end of one of the main weathering episodes. The weathering profile that developed on peridotite typically consists, from base to top, of bedrock, coarse saprolite, fine saprolite (yellow and red laterite), a nodular horizon and discontinuous iron crust. Saprolite is a permeable material that typically contains high levels of nickel due to the substitution of magnesium for nickel in serpentine by circulating surface waters. Both the regolith, which bears a world-class nickel resource, and the bedrock were deeply dissected by erosion during an episode of uplift, probably due to the late Oligocene slab break off (Sevin et al., 2014).

HIGH TEMPERATURE TRANSFER IN THE SUPRA-SUBDUCTION MANTLE

The harzburgite main body: petrological and geochemical data

Harzburgites of the New Caledonia Ophiolite are ultra-depleted rocks, lacking primary clinopyroxene and displaying some of the lowest trace element contents reported in mantle samples worldwide (Prinzhofer and Allègre, 1985; Bodinier and Godard, 2013). This extreme depletion reflects a polyphase melting history involving multiple episodes of melt extraction, possibly mediated by fluids. As a result, their geochemical characterization long remained challenging, until analytical advances in the 2000s enabled the acquisition of high-quality trace element and isotopic data (e.g., Marchesi et al., 2009; Ulrich et al., 2010; Pirard et al., 2013; Secchiari et al., 2020a).

To minimize the effects of elemental mobility related to serpentinization and/or tropical weathering, the geochemical and isotopic data of New Caledonian harzburgites were determined from fresh samples with minimal or very low serpentinization ratios (LOI = 0-3 wt.%). These harzburgites are spinel tectonites dominated by olivine and orthopyroxene and systematically lack primary clinopyroxene. Mineral chemistry consistently reflects their highly refractory character (Ulrich et al., 2010; Marchesi et al., 2009; Secchiari et al., 2020a). Olivine displays high Fo contents (90.7 to 92.6 mol.%), spinel shows elevated Cr# (0.440-0.715), and orthopyroxene is both Al-poor (1.30-2.73 wt.% Al_2O_3) and

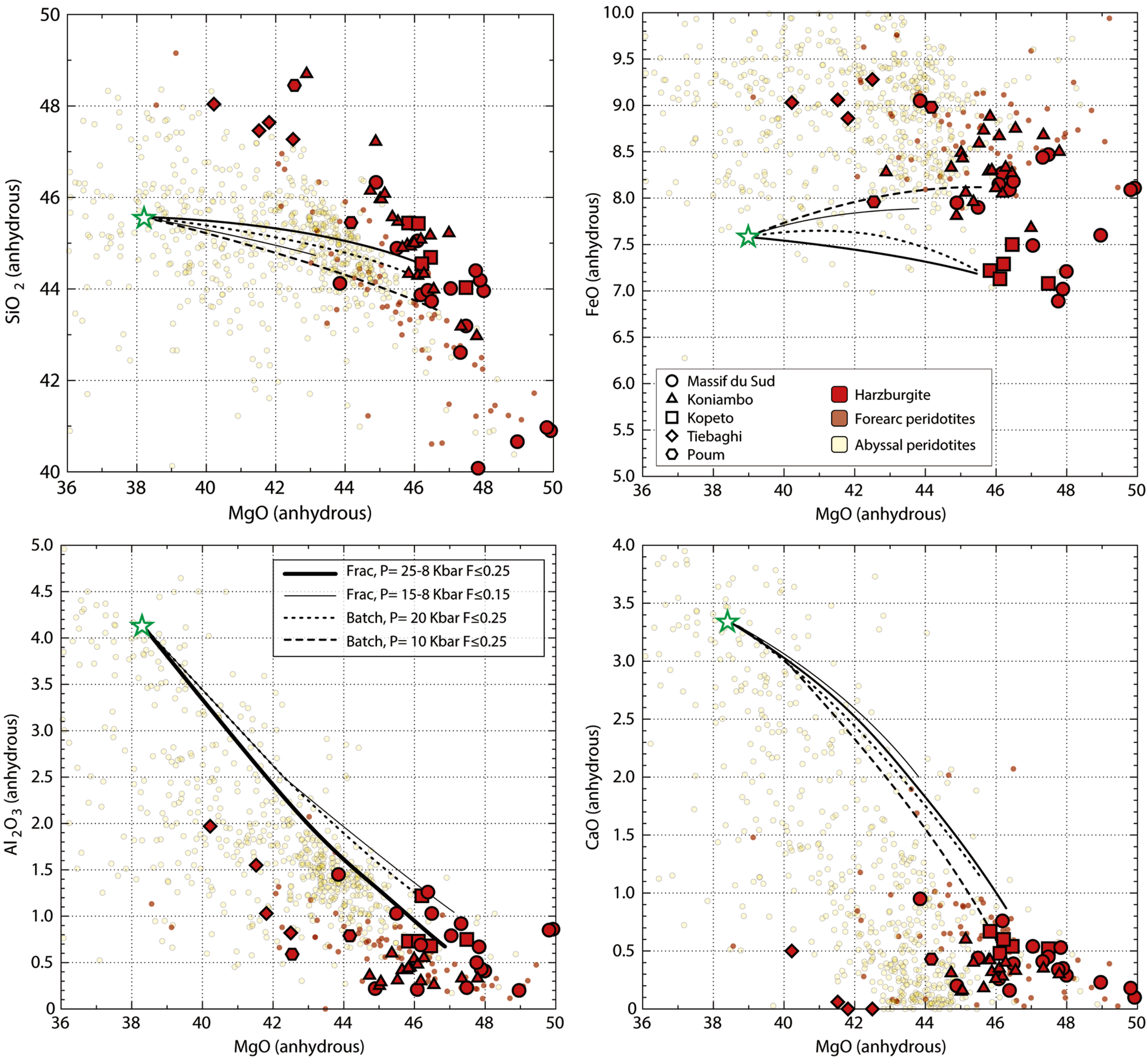

Fig. 2 - Bulk-rock abundances (calculated on an anhydrous basis) of SiO_2, FeO, Al_2O_3, and CaO of New Caledonia harzburgites. The calculated melting trends represent the compositional evolution of a residual peridotite applying the model of Niu (1997). New Caledonia harzburgite data are from Ulrich et al. (2010) and Secchiari et al. (2019).

characterized by high Mg# (Mg# = 0.914-0.924). Taken together, all these features are consistent with high degrees of melt extraction past clinopyroxene consumption.

Bulk-rock compositions display very low Al_2O_3 (0.41-1.21 wt.%), CaO (0.29-0.66 wt.%) and TiO_2 (≤0.01 wt.%) contents, coupled to elevated Mg# values (0.917-0.925). The MgO content ranges from 44.16 to 47.62 wt.%, and it is negatively correlated with SiO_2 (41.05 to 45.08 wt.%), as well as Al_2O_3, as predicted for mantle melting (Fig. 2).

On chondrite-normalized rare earth element (REE) patterns, all samples display extremely low REE contents (Fig. 3a), with concentrations ranging between 0.002 and 0.1 times chondritic abundances. With only a few exceptions, the harzburgites exhibit U-shaped patterns, characterized by strongly depleted HREE (DyN/YbN = 0.07-0.16) and fractionated LREE-MREE segments ((La/Sm)N = 2.22-8.30). Such U-shaped REE patterns cannot be generated by simple fractional melting, which typically produces concave downward chondrite-normalized REE profiles with flat HREE segments and depleted LREE. By contrast, U shaped REE patterns require selective LREE re-enrichment over MREE, implying the addition of an external component. This feature is commonly attributed to interaction with slab-derived fluids or melts in supra-subduction zone settings (Parkinson and Pearce, 1998).

Primitive-mantle (PM)-normalized trace element patterns further highlight the extreme depletion of these rocks (Fig. 3b), with most trace elements lying between 0.001- and 0.1-times PM abundances. Superimposed on these depleted patterns are small positive anomalies in fluid-mobile elements (FME; e.g., Cs, Ba, Sr), along with a pronounced Pb spike (up to 1000 times PM). Such enrichment patterns are commonly interpreted as evidence of interaction with slab-derived fluids, as Pb and other FME are preferentially mobilized during dehydration of altered oceanic crust and subducted sediments. The decoupling between enriched fluid-mobile elements and depleted high field strength elements is therefore characteristic of fluid-assisted melting in supra-subduction zone settings (Parkinson and Pearce, 1998; Bizimis et al., 2000).

Melting modeling and post-melting metasomatism

Major element variations (Fig. 2) indicate extremely high degrees of partial melting. Compared with anhydrous melting trends (Herzberg, 2004), the New Caledonia harzburgites display very low Al_2O_3 contents, consistent with melt extraction up to 25-30%. Similarly, geochemical modelling performed on whole-rock and orthopyroxene REE compositions points to very high degrees of partial melting (>25%), locally exceeding clinopyroxene exhaustion, of a depleted mantle source within the spinel stability field (Marchesi et al., 2009; Ulrich et al., 2010; Secchiari et al., 2020a). Such elevated melt extraction rates are difficult to reconcile with one single melting event and are best-explained by a two-stage evolution, involving an initial episode of dry melting, followed by fluid-assisted melting in a forearc setting (Secchiari et al., 2020a).

Despite their extremely low HREE contents, the New Caledonia harzburgites exhibit systematic enrichments in incompatible trace elements, including LREE, MREE, Nb, Zr, Hf and fluid-mobile elements (FME) such as Ba, Sr and Pb, both for whole rock (Fig. 3b) and orthopyroxene. These enrichments cannot be explained by melt depletion alone. In particular, while HREE abundances are well reproduced by high-degree melting models, concentrations of LREE-MREE and some HFSE are significantly higher than predicted for a purely residual composition. This decoupling indicates that the mantle residue was subsequently modified by interaction with supra-subduction zone fluids and melts.

Geochemical modelling shows that FME enrichment can be accounted by slab input during fluid-assisted melting (Secchiari et al., 2020a), consistent with observations from other modern and fossil forearc mantle sequences (e.g. Parkinson and Pearce, 1998; Shervais and Jeans, 2012; Jean and Shervais, 2017). However, additional processes are required to explain the abundances of the other incompatible trace elements. In the New Caledonia harzburgites, selective enrichments in incompatible elements, such as MREE, Nb, Zr, Hf, are closely associated with the occurrence of thin films of interstitial ortho- and clinopyroxenes (Secchiari et al., 2020a) and spinel-pyroxene symplectitic intergrowths (Secchiari et al., 2019).

The presence of thin films of orthopyroxene, characterized by low Al_2O_3, CaO and Cr2O3, has been often documented in arc xenoliths (Arai et al., 2004; Ishimaru et al., 2007; McInnes et al., 2001). These films are interpreted as products of mantle wedge metasomatism operated by either SiO_2-rich slab-derived aqueous fluids (containing a dissolved

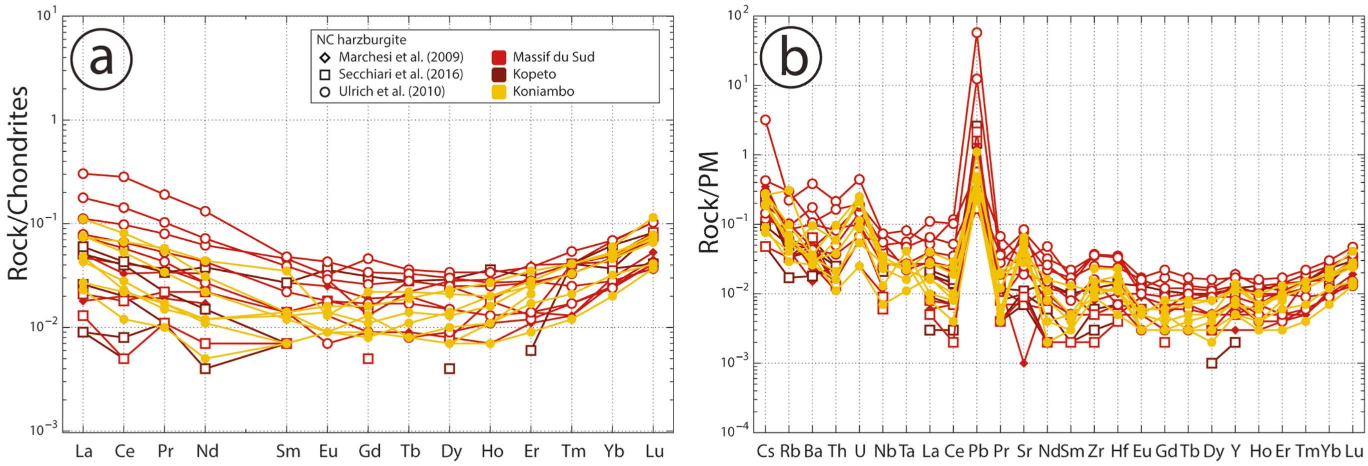

Fig - 3. a) Chondrite-normalized REE patterns showing the REE enrichment of moderately serpentinized harzburgites (circle and diamond symbols; Marchesi et al., 2009; Ulrich et al., 2010) compared to the U-shaped unserpentinized ones (square symbols; Secchiari et al., 2019); b) Extended trace elements patterns normalized to the Primitive Mantle showing the enrichment in FME relative to REE (Secchiari et al., 2019). The color chart refers to the sampling locations.

silicate component) or by hydrous silicate melts. Taken together, these petrographic and geochemical features support a scenario in which a highly depleted mantle residue was subsequently overprinted by local melt addition during forearc evolution. Although these subduction-related contributions are clearly recorded, geochemical modelling indicates that the addition of incompatible elements was quantitatively limited (Secchiari et al., 2020a).

Radiogenic Sr-Nd-Pb isotopes further constrain the evolution of the New Caledonia harzburgites. Age-corrected (53 Ma) Sr and Nd isotopic compositions (Fig. 4) display a wide range of compositions, from depleted MORB-like signatures to enriched, sediment-like values (Secchiari et al., 2020a). Initial $^{143}Nd/^{144}Nd$ ratios span from 0.51253 to 0.51278, while $^{87}Sr/^{86}Sr$ ratios range between 0.70257 and 0.70780. This variability indicates mixing between a depleted mantle source and an enriched component. The careful selection of fresh samples

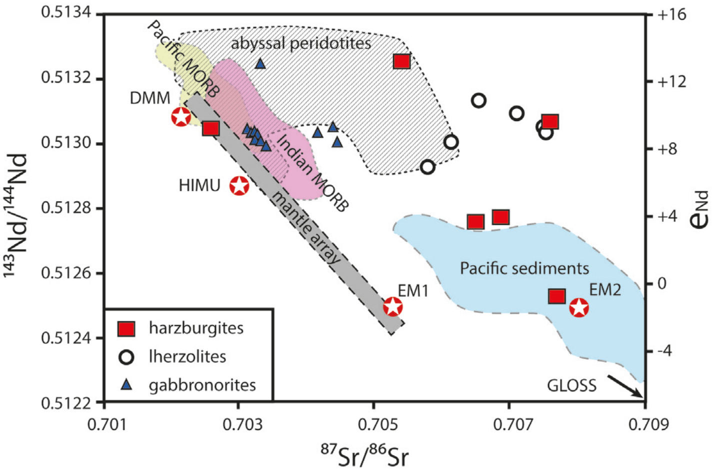

Fig. 4. - Age-corrected (53 Ma), $^{87}Sr/^{86}Sr$ vs. $^{143}Nd/^{144}Nd$ diagram for the New Caledonia ophiolitic rocks. Lherzolites and gabbronorites data are from Secchiari et al. (2016) and Secchiari et al. (2018), respectively. Redrawn from Secchiari et al. (2019).

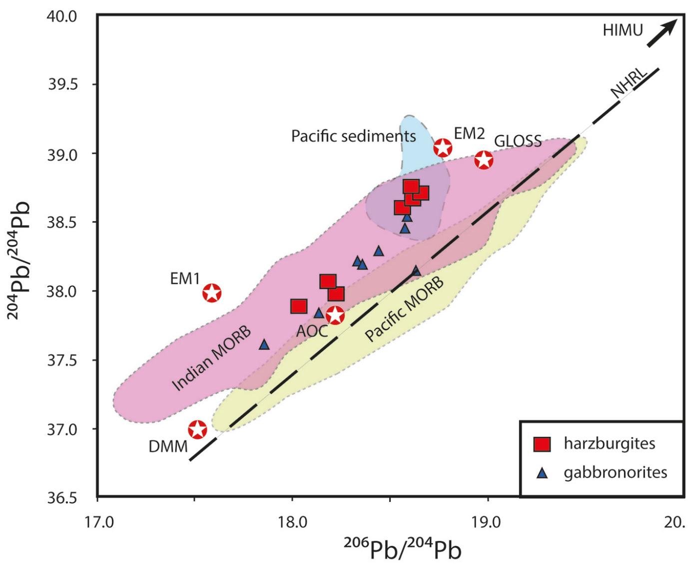

Fig. 5 - Age-corrected (53 Ma) $^{206}Pb/^{204}Pb$ vs. $^{208}Pb/^{204}Pb$ for the New Caledonia harzburgites. New Caledonia lherzolites and gabbronorites data are after Secchiari et al. (2016) and Secchiari et al. (2018). Redrawn from Secchiari et al. (2019).

excludes significant alteration effects, ruling out seawater interaction as the cause of the isotopic signatures. Instead, the enriched component is best explained by contributions from subducted sediments and/or slab-derived fluids.

Pb isotopes further support this interpretation. Initial $^{206}Pb/^{204}Pb$, $^{207}Pb/^{204}Pb$, and $^{208}Pb/^{204}Pb$ ratios range from 18.038 to 18.638, 15.455 to 15.642, and 37.920 to 38.731, respectively. In the $^{208}Pb/^{204}Pb$ vs. $^{206}Pb/^{204}Pb$ space, the samples overlap the field of Indian-type MORB and define a positive trend, with some samples extending into the Pacific sediment field (Fig. 5). Other samples display intermediate compositions between DMM and EM2 end-members. In the $^{206}Pb/^{204}Pb$ vs. $^{207}Pb/^{204}Pb$ space (not shown), the data are more scattered but generally show elevated $^{207}Pb/^{204}Pb$ ratios, again consistent with sediment involvement (Secchiari et al., 2020a). Overall, the isotopic variability indicates incorporation of a sediment-derived component into the mantle source, consistent with metasomatic modification in a forearc setting.

Re-Os systematics add a further dimension to this evolution (Secchiari et al., 2020b). The harzburgites display subchondritic to variably radiogenic initial $^{187}Os/^{188}Os$ ratios, defining two distinct highly siderophile elements (HSE) groups and yielding model ages locally exceeding 1 Ga. These signatures indicate that portions of the mantle experienced ancient melt depletion events, predating the Eocene evolution, and that this long-lived depleted signature was only partially overprinted by later subduction-related processes.

Taken together, these observations are consistent with the geodynamic evolution of the SW Pacific region, which involved marginal basin opening during the Late Cretaceous-Paleocene followed by intra-oceanic subduction during the Eocene (e.g., Cluzel et al., 2001, 2012, 2016). The relatively limited enrichment in fluid-mobile elements is consistent with subduction of young oceanic lithosphere, characterized by low sediment input.

Near-ridge and suprasubduction melt re-enrichment of the Tiebaghi lherzolite

Lherzolites constitute a volumetrically minor yet petrologically critical component of the New Caledonia Peridotite Nappe, whose mantle section is otherwise dominated by strongly depleted harzburgites. Their geological significance has been progressively clarified over the last four decades, evolving from early models of sequential melting to recent multi-isotope constraints revealing the involvement of ancient mantle domains. Collectively, these studies document a complex evolution including melting at a mid-ocean ridge setting, localized melt-rock interactions, and subsequent incorporation into a forearc setting during subduction initiation.

Early investigations emphasized the structural and stratigraphic context of lherzolite bodies within the northern klippes of the Peridotite Nappe (Fig. 1). Mapping of peridotite massifs and chromite-bearing sequences (Moutte, 1982; Leblanc and Violette, 1983) has shown that lherzolites systematically overlie dunites and harzburgites with their contacts commonly marked by transitions enriched in Cr-rich spinel. These observations highlighted their fertility relative to the dominant harzburgites but did not firmly establish their mantle origin. A first explanatory framework emerged from petrostructural and petrochemical studies: Seicher (1981) identified a large-scale shear zone extending from Belep Island to the Tiébaghi Massif, interpreted as a paleo-oceanic transform fault. In this context, Nicolas and Dupuy (1984) proposed that the New Caledonia lherzolites represent a secondary facies derived from harzburgitic protoliths through melt percolation and local melt trapping. In parallel, Prinzhofer and Allègre (1985) introduced a polybaric, sequential melting model to explain the REE patterns of New Caledonia peridotites. Their model invokes progressive melting of a mantle column from the garnet to the plagioclase stability fields, producing a vertical sequence in which strongly depleted harzburgites overlie more fertile lherzolites. In this framework, they interpreted the lherzolite-harzburgite association as reflecting spatial variations in melting degree within a mantle section.

A major conceptual shift occurred with the work of Ulrich et al. (2010), who demonstrated that the New Caledonia lherzolites originated as abyssal peridotites formed at a spreading ridge and subsequently modified by limited, near-in situ refertilization. Their major-element systematics, and clinopyroxene trace elements compositions, together with spoon-shaped REE patterns – reflecting partial melting followed by limited re-equilibration with percolating melts –, indicate moderate degrees (5-15%) of MOR-type melting during the Late Cretaceous. These features further imply subsequent interaction with MORB-like melts responsible for the formation of plagioclase-lherzolite facies. The study of Ulrich et al (2010) established the now widely accepted interpretation that the New Caledonia lherzolites represent pre-forearc, ridge-derived mantle, in marked contrast to the harzburgites, which record supra-subduction hydrous melting associated with Eocene subduction initiation.

High-resolution geochemical and isotopic studies conducted in the 2010s further refined this interpretation. Secchiari et al. (2016) showed that the lherzolites display moderately depleted abyssal-type signatures, consistent with residues of moderate melting, as indicated by the presence of 7-8 vol.% clinopyroxene and relatively low bulk-rock Al_2O_3 and CaO contents (Fig. 6).

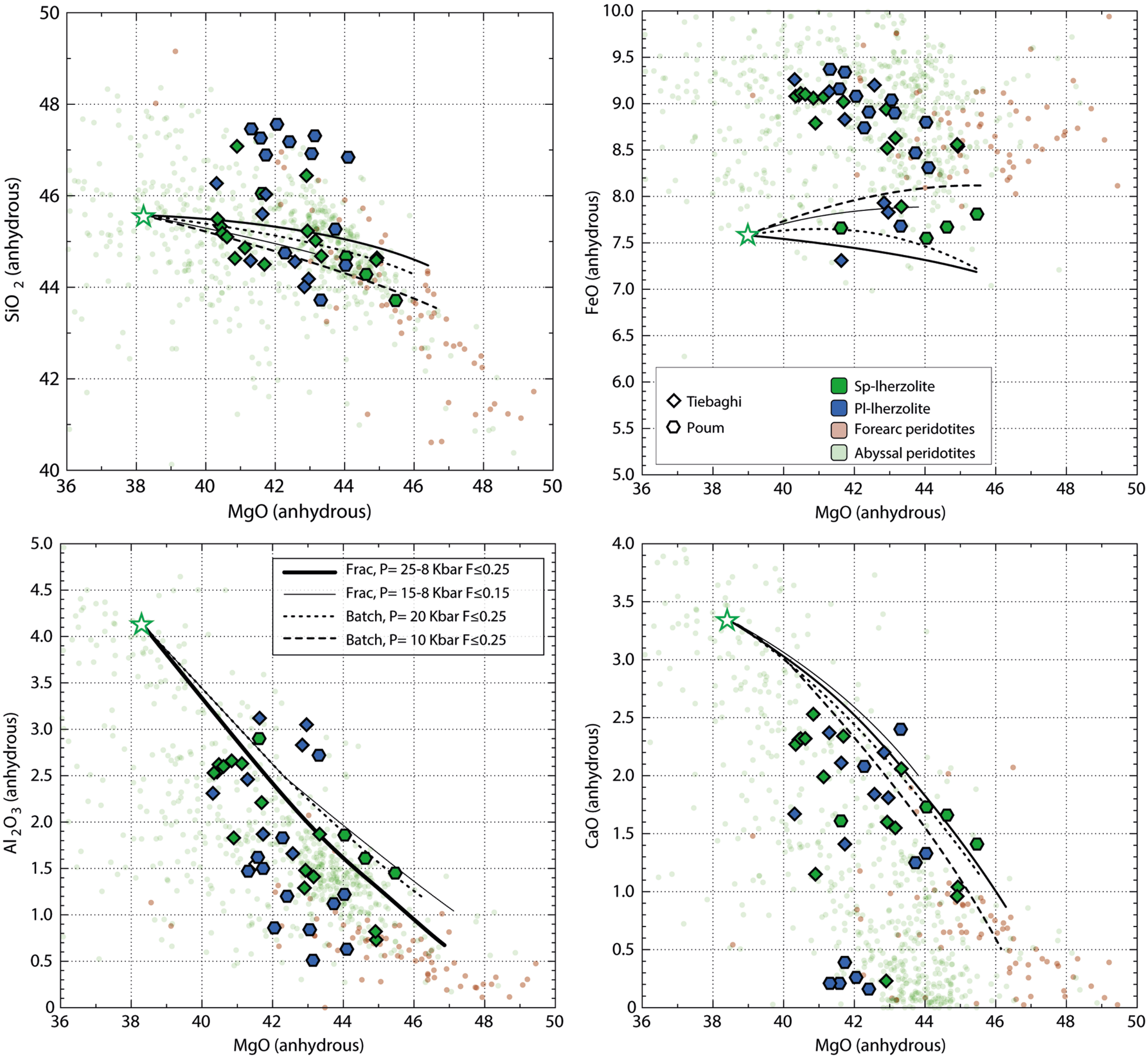

Fig. 6 - Bulk-rock abundances (calculated on an anhydrous basis) of SiO_2, FeO, Al_2O_3, and CaO of New Caledonia lherzolites. The calculated melting trends represent the compositional evolution of a residual peridotite applying the model of Niu (1997). New Caledonia lherzolite data are from Ulrich et al. (2010), Secchiari et al. (2016), and Cai et al. (2022). Abyssal and forearc peridotites are the same as in Fig. 2.

Clinopyroxene compositions vary systematically with facies: spinel-facies porphyroclasts contain higher Na_2O (~0.50 wt.%) and lower Cr_2O_3 (<1 wt.%) than those of plagioclase-facies lherzolites (Na_2O ~0.3 wt.% and Cr_2O_3 ~1.3 wt.%). These compositional differences reflect variations in melting conditions and subsequent melt-rock interaction during lithospheric evolution.

In particular, the REE patterns (Fig. 7a) indicate that spinel-lherzolites formed after ~8-10% partial melting initiated in the garnet stability field (Secchiari et al. (2016). These authors further showed that plagioclase lherzolites record cryptic melt entrapment, involving infiltration of strongly depleted MORB-type melts into the shallow lithospheric mantle. Sr-Nd isotopic compositions indicate derivation from an asthenospheric mantle source that underwent a MORB-like depletion event, followed by only limited subsequent re-enrichment shortly before the Eocene in a marginal-basin setting.

The lherzolites exhibit subchondritic to slightly suprachondritic initial $^{187}Os/^{188}Os$ (0.1273-0.1329) and PM-normalised HSE abundance diagrams characterised by gently sloping patterns showing increasing depletion towards Re-Au, consistent with low to moderate melt extraction in a MOR setting (Liu et al., 2019; Secchiari et al., 2020a). Late-stage seawater-rock reactions also led to high and variable sulfur contents (202-1268 ppm) in the lherzolites (Secchiari et al., 2020a). These signatures sharply contrast with the extreme HREE depletion and heterogeneous Os isotopes observed in the New Caledonia harzburgites (Secchiari et al., 2020b), reinforcing the distinction between these two mantle domains and implying the juxtaposition of mantle blocks with different depletion histories.

A further conceptual advance came from mineral-scale Lu-Hf isotope analyses. Xu et al. (2022) showed that some lherzolites have highly radiogenic initial Hf isotope ratios coupled with unradiogenic Os signatures, implying ancient depletion ages (0.5-1.5 Ga), despite their relatively young Nd isotopic compositions. Such decoupling indicates that Hf and Os preserved ancient depletion signatures, whereas Nd isotopes and trace-element characteristics were reset during more recent melt-rock interactions, reflecting the different sensitivities of these isotope systems to melting and metasomatic processes. These results suggest that the New Caledonia lherzolites incorporate fragments of ancient, pre-Eocene depleted asthenosphere that were subsequently involved in forearc formation during subduction initiation.

In a recent contribution, Cai et al. (2025) provide mineralogical and geochemical constraints that further support this interpretation. Their study of platinium group elements (PGE) systematics reveals pronounced enrichment in Pt-Pd relative to Os-Ir-Ru as well as elevated (Pt/Ir)n and (Pd/Ir) n ratios in the lherzolites from the Tiébaghi massif. Such signatures cannot be produced by partial melting alone and instead require the addition of PGE-enriched, S-saturated melts, which introduced interstitial sulfides and chalcophile elements and overprinted the primary abyssal HFSE signature. The major advance of Cai et al. (2025) is the first set of Ca isotope measurements on these peridotites, which provide strong constraints on the nature of the metasomatic agent. The lherzolites display a restricted range of $\delta^{44/40}Ca$ values systematically lower than those typically assumed for the upper mantle (Chen et al., 2018, 2019). Because serpentinization does not fractionate Ca isotopes and partial melting produces only minimal isotopic effects, these light $\delta^{44/40}Ca$ values, systematically lower than typical upper mantle values, must be inherited from an infiltrating melt. Carbonate-rich melts derived from subducted marine carbonates – characterized by intrinsically light Ca isotope compositions (Fantle and Tipper, 2014a, b) – therefore represent the most plausible source. Positive correlations between $\delta^{44/40}Ca$ and CaO, as well as between $\delta^{44/40}Ca$ and Ce/Eu ratios, further support mixing between the mantle residue and a Ca-rich, carbonate-bearing melt, providing strong evidence for carbonate-derived metasomatism during the earliest stages of subduction initiation.

Taken together, the New Caledonia lherzolites represent pre-forearc mantle residues formed by moderate degrees of MOR-type melting, subsequently modified by shallow melt infiltration, and incorporated into a forearc setting during rapid Paleocene-Eocene subduction initiation. Thermal modelling (Secchiari et al., 2022a) is consistent with this evolution: high closure temperatures (>1200 °C based on REE thermometry; Secchiari et al., 2022a; Xu et al., 2022) and rapid cooling rates (~10^{-3} °C/yr) indicate that the lherzolites were accreted from upwelling asthenosphere into a nascent

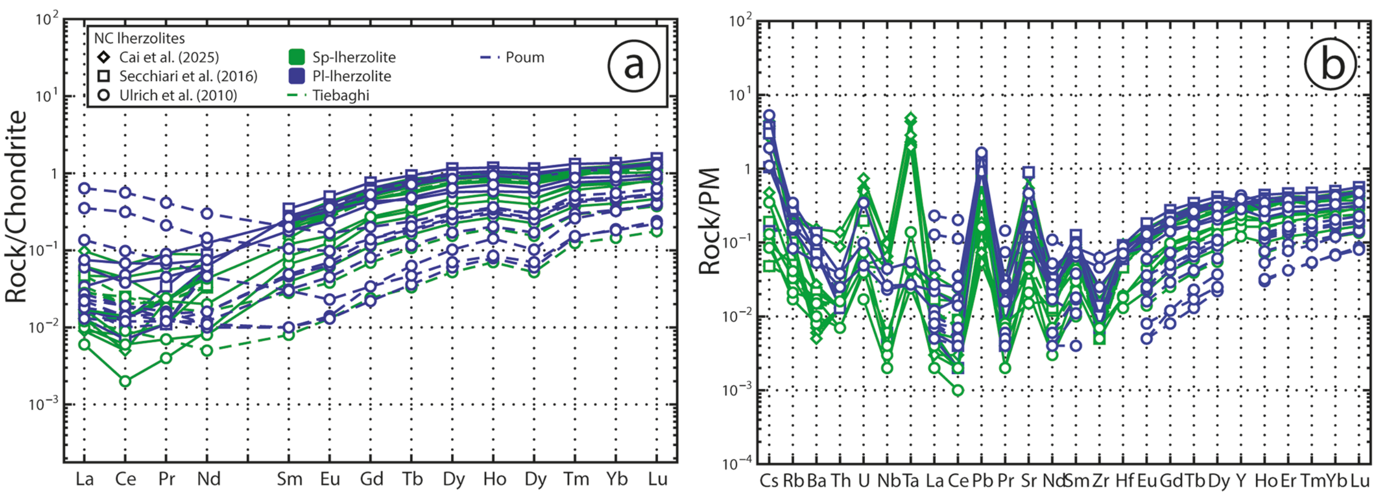

Fig. 7 - (a) Chondrite-normalized REE patterns of spinel- and plagioclase-lherzolites from the northern massifs (Tiebaghi and Poum) highlighting spoon-shaped distributions. (b) Primitive mantle (PM)- normalized trace element patterns. Data from Ulrich et al. (2010), Secchiari et al. (2016), and Cai et al. (2022).

forearc lithosphere and cooled rapidly enough to preserve their magmatic REE signatures. Combined elemental, isotopic and PGE heterogeneities attest to the juxtaposition of young MORB-source asthenosphere, ancient depleted mantle domains, and forearc-related metasomatic imprints, thereby providing an exceptional record of mantle processes operating during the transition from oceanic (forearc) spreading to incipient subduction.

The mantle-crust transition zone and crustal section of the New Caledonia ophiolite

Prinzhofer et al. (1980), Nicolas and Prinzhofer (1983) and Pirard et al. (2013) described in details the structure of the mantle-crust transition zone (MTZ) and crustal section of the New Caledonia ophiolite, which crop out in several areas of the Massif du Sud (Naoué, Montagne des Sources, Col de Mouirange, Rivière des Pirogues, Plum, Prony and Ile Ouen) (Fig. 8).

In this massif, the mantle section consists of harzburgites locally interlayered with dunite and orthopyroxene-rich lenses, or cut by pyroxenite, diabase and gabbroic dikes. The transition from mantle tectonites to the MTZ is irregular and progressive in the field, extending over about ~300 m in thickness. Up-section within the tectonites, dunite bands become increasingly abundant and thicker, eventually isolating bodies of orthopyroxene-poor harzburgites with sharp contacts and interfingering relationships with the surrounding dunites. From bottom to top, the MTZ consists of massive dunites locally enclosing small chromitite pods, followed by clinopyroxene/plagioclase-bearing dunites, wehrlites and pyroxenites, in contact with upper gabbronorite and gabbro sills (Fig. 9). These upper mafic lithologies constitute the lower oceanic crust, whereas middle and upper crustal rocks are absent, possibly due to deep erosion or tectonic detachment (Cluzel et al., 2001).

Compared to harzburgites, dunites have higher Al_2O_3 (0.54-0.88 anhydrous wt.%) and CaO (0.27-0.87 anhydrous wt.%) contents reflecting local precipitation of small amounts of clinopyroxene and plagioclase. (Marchesi et al., 2009). Wehrlites are significantly more enriched in these components (Al_2O_3 = 0.93-4.59 wt.%, CaO = 1.40-4.06 wt.% anhydrous) and display a well-defined positive correlation between Al_2O_3 and CaO, consistent with increasing modal abundances of these phases (Marchesi et al., 2009).

Dunites have similar LREE-MREE and higher HREE contents than harzburgites (~ 0.02-0.2 x chondrite). They show flat to concave-upward LREE segments, positive Eu anomalies (Eu*= 3.0-4.7) and less fractionated HREE segments (Marchesi et al., 2009). Wehrlites have higher REE than dunites (~ 0.02-0.2 for LREE and 0.1-1 for HREE x chondrite) and normalized patterns with positive Eu anomalies (Eu*= 1.0-2.8) (Marchesi et al., 2009). Their REE variability reflects the heterogeneous modal ratios between olivine and clinopyroxene, along with the occurrence of plagioclase. PM-normalized incompatible trace element patterns of dunites generally have prominent Pb and Sr positive anomalies (Marchesi et al., 2009). Wehrlites are richer in incompatible trace elements than dunites, and their normalized patterns normally show negative anomalies of HFSE and positive anomalies of Pb and Sr (Marchesi et al., 2009).

Based on field structures, textures, and mineral compositions, both Nicolas and Prinzhofer (1983) and Pirard et al. (2013) interpreted the well-developed dunite section of the New Caledonia ophiolite as reflecting either magmatic accumulation or melt-rock interaction processes. Field relationships strongly support a replacive origin for the lowermost dunite layers in contact with mantle tectonites: their abundance increases progressively upward and they locally enclose harzburgite blocks with the same orientation od foliation, consistent with dunite formation by melt percolation and reaction (Nicolas and Prinzhofer, 1983). However, the dunite section is internally heterogeneous, with systematic variations in texture and mineral chemistry around the middle part of the MTZ. Up-section, textures evolve from porphyroclastic to equigranular, evidence of plastic deformation decreases,

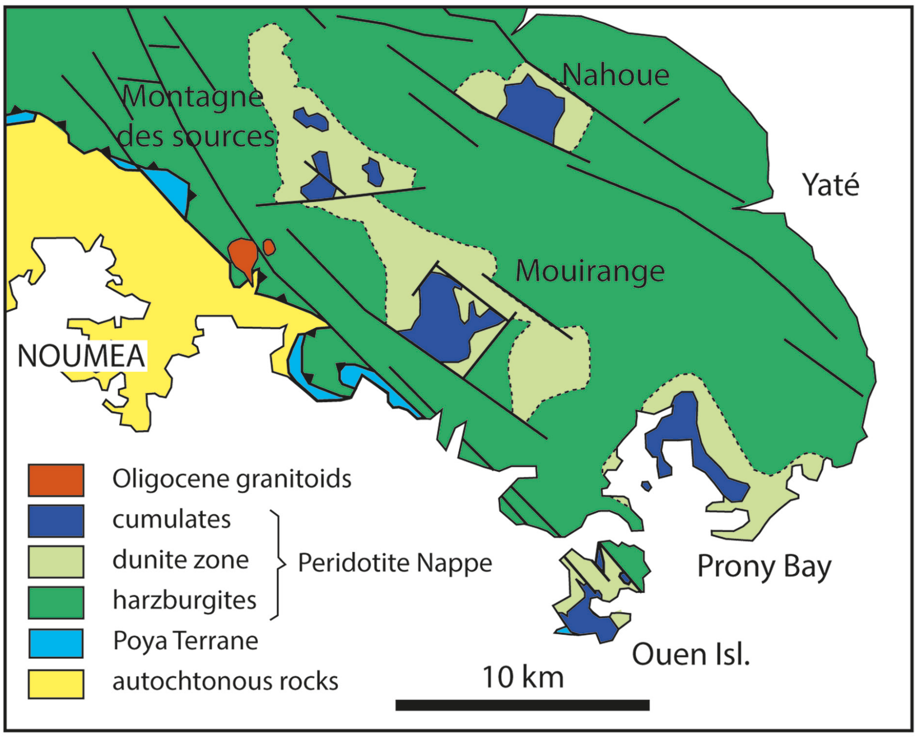

Fig - 8. Geological sketch map of the Massif du Sud showing the occurrences of the mantle-crust transition zone (redrawn and simplified from the online geological map of New Caledonia, DIMENC-SGNC-BRGM, 2010).

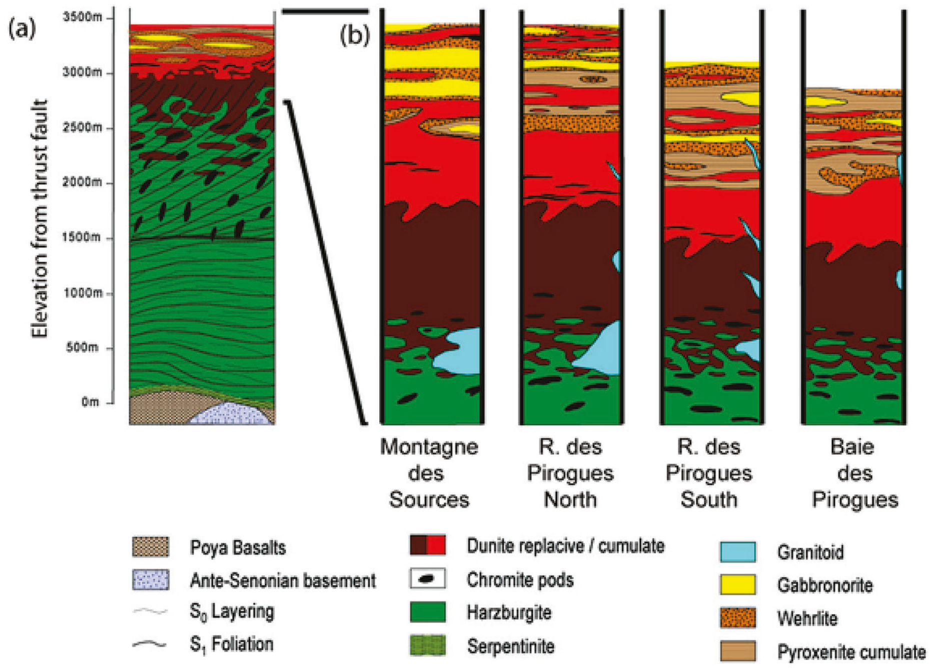

Fig. 9 - Details of the MTZ lithological sequences cropping out in the localities of Montagne des Sources, Rivière des Pirogues north and south, and Baie des Pirogues. The Figure is from Pirard et al. (2013).

olivine grains become more polygonal, and spinel habit shifts from vermicular to rounded, sub-idiomorphic forms. In addition, olivine Fo contents (89.5-90.7 mol.%) and Ni, V, and Cr concentrations, as well as spinel Cr#, are lower in the upper MTZ compared to deeper levels (where olivine Fo contents = 90.6-93.2 mol.%).

Pirard et al. (2013) interpreted these variations as recording a transition between two distinct genetic domains within the MTZ (each domain ~200-300 m thick). In their model, dunites in the lower half formed by percolation of orthopyroxene-undersaturated melts through mantle tectonites, inducing syntectonic recrystallization, olivine precipitation, and pyroxene dissolution (Kelemen, 1990). In contrast, dunites in the upper MTZ are interpreted as cumulates formed by crystallization of olivine and spinel from melts that interacted only minimally with the surrounding peridotites, as also inferred by Xu and Liu (2026). The boundary between these two domains is thus considered to represent the petrological paleo-Moho. Within this framework, clinopyroxene- and plagioclase-bearing dunites, together with associated wehrlites and pyroxenites in the upper MTZ (Fig. 9), are interpreted as products of magmatic accumulation of minerals precipitated from primitive, hydrous arc melts in the crust.

An alternative interpretation emphasizes the dominant role of melt-rock interaction throughout most of the MTZ. Nicolas and Prinzhofer (1983), while not excluding a cumulate origin for the uppermost ~200 m of the Montagne des Sources section, argued that the observed structural and textural features primarily reflect pervasive melt-rock reaction, with dunites forming through orthopyroxene dissolution in mantle tectonites. In this scenario, subsequent melt impregnation of these replacive dunites would account for the development of clinopyroxene- and plagioclase-bearing dunites and wehrlites. Consistently, Marchesi et al. (2009) interpreted wehrlites as products of melt-rock interaction, whereby discrete batches of different ultra-depleted, high-SiO_2 (boninite-like) melts percolated through pre-existing dunites and harzburgites, inducing olivine dissolution and the crystallization of clinopyroxene ± orthopyroxene ± plagioclase.

The lower crustal rocks (gabbronorites and orthopyroxene-gabbros) are uniformly primitive and refractory, with whole-rock Mg# values of 86.3-92.6 (Marchesi et al., 2009; Secchiari et al., 2018) and TiO_2 invariably <0.10 wt%. A large gap divides wehrlite from gabbronorite and orthopyroxene-gabbro compositions in terms of Al_2O_3 and CaO contents (Al_2O_3 = 13.61-23.92 and CaO = 12.61-18.44, on anhydrous basis in wt.%). Mineral compositions reinforce their primitive character, with extremely calcic plagioclase (An90-96 mol%), high-Mg# and Al-poor clinopyroxene, and olivine with forsterite contents between 87-89 mol %. The application of different geobarometers and geothermometers constrains the conditions of mineral precipitation in gabbronorites at P = 0.2-0.4 GPa and T = 1100-1300 °C (Pirard et al., 2013; Secchiari et al., 2018; Secchiari et al., 2022a).

Chondrite-normalized whole-rock REE patterns are strongly depleted in LREE, exhibiting concave-upward LREE segments, very low absolute REE abundances, nearly flat HREE distributions and low Yb_N (0.10-1.10 x chondrite). All samples display pronounced positive Eu anomalies (Eu* ≈ 1.6-3.3), reflecting plagioclase accumulation. Clinopyroxene trace element patterns closely mirror the whole-rock depletion (Marchesi et al., 2009; Secchiari et al., 2018). Extended incompatible trace element patterns further highlight this geochemical signature with concentrations mostly between 0.01 and 1 × PM, coupled with enrichments in fluid-mobile elements (Cs, Rb, Ba) and pronounced positive Pb and Sr anomalies. These features point to a composite geochemical signature recording both extreme melt depletion and selective enrichment by slab-derived fluid-mobile components.

Secchiari et al. (2018) analyzed the whole-rock Sr-Nd-Pb isotopic compositions of gabbronorites from different localities. They report age-corrected (53 Ma) $^{143}Nd/^{144}Nd$ ranging between 0.51299 and 0.51324 (8.16 ≤ εNdi ≤ 13.13), and $^{87}Sr/^{86}Sr$ between 0.703115 and 0.704443. Initial ^{206}Pb/204Pb span from 17.857 to 18.632, $^{207}Pb/^{204}Pb$ from 15.468 to 15.601, and $^{208}Pb/^{204}Pb$ from 37.608 to 38.540 (Fig. 4 and Fig. 5). These values generally overlap with those of Pacific and Indian MORB.

Mineral and whole-rock compositions of gabbronorites and orthopyroxene-gabbros located above wehrlites/pyroxenites (Fig. 9) indicate that they were produced by accumulation of pyroxenes and plagioclase from mantle-derived melts. However, major and trace element signatures of minerals and whole-rocks are more depleted in REE and HFSE compared to gabbroic cumulates from both mid-ocean ridges and island arcs (Marchesi et al., 2009; Secchiari et al., 2018). These authors interpreted the New Caledonia gabbronorites as lower crustal cumulates formed from primitive, ultra-depleted melts. These melts resemble the peculiar, Amami Sankaku Basin basalts erupted during the early development of the Izu-Bonin Mariana Arc (Li et al., 2021). The inferred mantle source was a depleted MORB mantle (DMM) that had previously undergone significant melt extraction. This mantle was subsequently metasomatized by slab-derived fluids, which introduced fluid-mobile elements (e.g., Ba, Sr, Pb) (Secchiari et al. 2018). Although the gabbronorite-forming melts share some features with boninites (high Mg#, strong depletion in REE, fluid-mobile element enrichment), they differ from boninites by having lower LREE-MREE abundances and lacking typical Nb depletion or Zr-Hf enrichment. Importantly, these rocks did not form from a large, homogenized magma reservoir. Instead, they represent the emplacement of small, non-aggregated magma batches, preserving the chemical variability and depletion of individual melt pulses (Secchiari et al., 2018).

Overall, the MTZ and lower crustal section of the New Caledonia ophiolite record a complex interplay between melt-rock interaction and magmatic accumulation processes during the earliest stages of subduction initiation. The MTZ documents the progressive evolution from replacive dunite formation in mantle tectonites to magmatic, cumulate assemblages upward, marking the transition to crustal conditions. Crystallization of hydrous, boninite-like melts occurred during the early stages of the arc igneous activity when extensional tectonics dominates the forearc region similar to regimes at mid-ocean ridges (Stern, 2004). The overlying gabbronorites and orthopyroxene-gabbros are products of the crystallization of primitive, ultra-depleted melts derived from a highly refractory mantle source variably modified by slab-derived fluids. Their geochemical signatures – combining extreme REE depletion with selective enrichment in fluid-mobile elements – highlight the role of small, non-aggregated melt batches and provide key insights into the generation of nascent fore-arc crust in a supra-subduction setting.

The Lower Eocene dikes (55-50 Ma): melt variability during hot subduction initiation

Dikes and sills with supra-subduction characteristics are found at any level of the New Caledonia ophiolite, i.e., within the main harzburgite-dunite body, but also in the cumulate layers, and as blocks in the tectonic sole made of mylonitic serpentinite. In the latter, the dikes are severely fractured and display boudinage, while they are well preserved in the rest of the ophiolite. Geochemically similar blocks of magmatic rocks with 55-50 Ma U-Pb zircon ages are also found in serpentinite mélanges of the HP-LT belt in northern New Caledonia(Cluzel, 2020). Most mafic and felsic intrusive rocks are medium- to coarse-grained and locally display pegmatitic texture; in contrast, boundary features such as the chilled margins of the dolerite dikes and the thin, low-temperature reaction aureoles (comprising tremolite, talc, chlorite, and serpentine) developed around some felsic dikes unambiguously indicate that magma intruded into peridotite and cumulates that were progressively cooling. Some dikes underwent internal ductile deformation (i.e., mineral boudinage, mineral preferred orientation, flow folding or microfolding, mylonitization), which is not observed in the peridotite host. A compositional layering parallel to dike walls is locally developed, thus suggesting high-temperature shearing and magma injection into active faults (Cluzel, 2020).

Dikes are prominently diverse and their mineral modes vary from ultramafic (pyroxenite) to mafic (gabbro, diorite, hornblendite, dolerite, boninite) to felsic (leucogabbro, leucodiorite, granite). Post-magmatic alteration is evidenced in some rocks by the variability of mobile elements and occurrence of secondary mineral phases (tremolite, chlorite, etc). Winchester and Floyd's (1977) classification diagram based on "immobile" elements shows a relatively wide array (Fig. 3S), which precludes a single differentiation trend. Two main types of pyroxenites intruded into the New Caledonia peridotites: one single kilometer-sized intrusion (Plum pyroxenite) and centimeter-thick dikelets in the whole unit (e.g., Bogota peninsula harzburgites).

Plum pyroxenite intrusion

The Plum composite intrusion in the Massif du Sud consists of a subcircular pyroxenite body about 2 km wide and some smaller elliptical bodies intruded in strongly serpentinized harzburgites near the base of the ophiolite. It forms roughly concentric envelopes with dunite, wehrlite, and websterite inwards. The pyroxenite is in turn intruded by hornblende-gabbronorite dikes oriented either parallel to the curved shape of the intrusion or perpendicularly crosscutting it. Some dikes are sheared and mylonitized. The overall Z-shaped structure, with directions changing eastward from E-W to N-S and E-W, and partitioned internal foliation, suggests synkinematic intrusion in a dextral transcurrent setting (Cluzel et al., 2024). The main petrographic and geochemical features of the Plum pyroxenite have been investigated in detail by Secchiari et al. (2022b), and will only be summarized here. The pyroxenite body consists of medium-grained websterites mainly composed of orthopyroxene (~ 30-75 vol %) and Al_2O_3 and TiO2-poor clinopyroxene (~ 20-50 vol.%), coupled to variable amounts of amphibole (~ 2-20 vol.%) and minor plagioclase (up to 9 vol.%) with highly calcic composition (An88-An96). Gabbronorite dikes show variable grain size. Mineral modes of the dikes are characterized by lower pyroxene contents (Opx ~ 3-40 vol %; Cpx ~ 5-25 vol %) together with higher amphibole and plagioclase abundances (~20-30 vol % and ~10-55 vol %, respectively) compared to the main pyroxenite body. Pale green amphibole mainly occurs as an interstitial phase texturally associated with clinopyroxene. Abundant amphibole blebs, with rounded or irregular margins, are commonly found within clinopyroxene, often in optical continuity with the interstitial amphibole. The amphibole may also form rims on clinopyroxene. According to Secchiari et al. (2022b), the amphibole crystallization may be ascribed to replacement reactions involving the early-crystallized clinopyroxene in a crystal mush environment. Despite the slightly different mineral modes, in situ major element investigation revealed similar compositional features for the pyroxenite core and the crosscutting dikes. The pyroxenite intrusion and the associated dikes register similar equilibrium temperatures, thus implying a common cooling history (Secchiari et al., 2022 a, b).

$^{40}Ar/^{39}Ar$ ages have been obtained for magnesio-hornblendes from a websterite and a gabbro dike. The hornblendes from websterite yield a well-defined plateau age of 52.3 ± 0.6 Ma while those from the gabbro sample have a much older apparent age (70 to 60 Ma) due to excess argon; however an isochron array yields an age of 53.9 ± 0.6 Ma. These isochron dates are within the range of U-Pb zircon ages of hornblende-bearing gabbro and diorite dikes (55.6-50.0 Ma) (Cluzel et al., 2006; 2024).

The Plum pyroxenites are depleted in incompatible elements and display negative Nb, Zr, Hf, Ta and Ti anomalies on MORB-normalized trace element diagrams (Fig. 10). The associated dikes are slightly more depleted and display Eu-positive anomalies that suggest plagioclase segregation. Geochemical modelling based on whole-rock and clinopyroxene trace element compositions indicates that putative melts in equilibrium with the Plum intrusives have a geochemical signature strongly recalling those of the clinoenstatite-bearing (CE) boninites of Népoui (west coast of New Caledonia; Cluzel et al., 2016; Secchiari et al., 2022b) (Fig. 10a, b).

Pyroxenite dikelets from the Bogota Peninsula

The Bogota Peninsula ultramafic rocks represent the NW extension of the Massif du Sud along the northeastern coast of New Caledonia (Fig. 1b). The orientation of the peridotite layering varies throughout the Bogota Peninsula from E-W to N-S, dipping 35° to 65°; a stretching lineation marked by chromite streaks and elongated/boudinaged orthopyroxene grains with a pitch of about 45° in any direction is also observed. The moderately dipping layering connects to, or is crosscut by, high-temperature dextral shear zones defined by steep mylonitic foliation bearing a shallow dipping lineation. The main shear zone was interpreted as an ancient oceanic transform fault and referred to as Bogota Transform Fault (BTF) (Prinzhofer and Nicolas, 1980; Titus et al., 2011). BTF is about 2 km wide around the Ouassé Village, while narrower high-strain zones are found elsewhere; a secondary shear zone was also described 20 km to the NW near Kouaoua Village (Titus et al., 2011). However, this interpretation was challenged in view of the overall tectonic characteristics of New Caledonia and shear zone repartition during the Eocene and a model of transcurrent syn-subduction tectonics was suggested instead (Cluzel et al., 2021).

A number of ultramafic-mafic dikes are distributed throughout the peninsula. Although they are widely spaced, often preventing crosscutting relationships from being observed, the relative timing from earliest to latest was suggested to be pyroxenite, plagioclase-bearing pyroxenite, hornblende gabbro and dolerite/basalt (Prinzhofer and Nicolas,

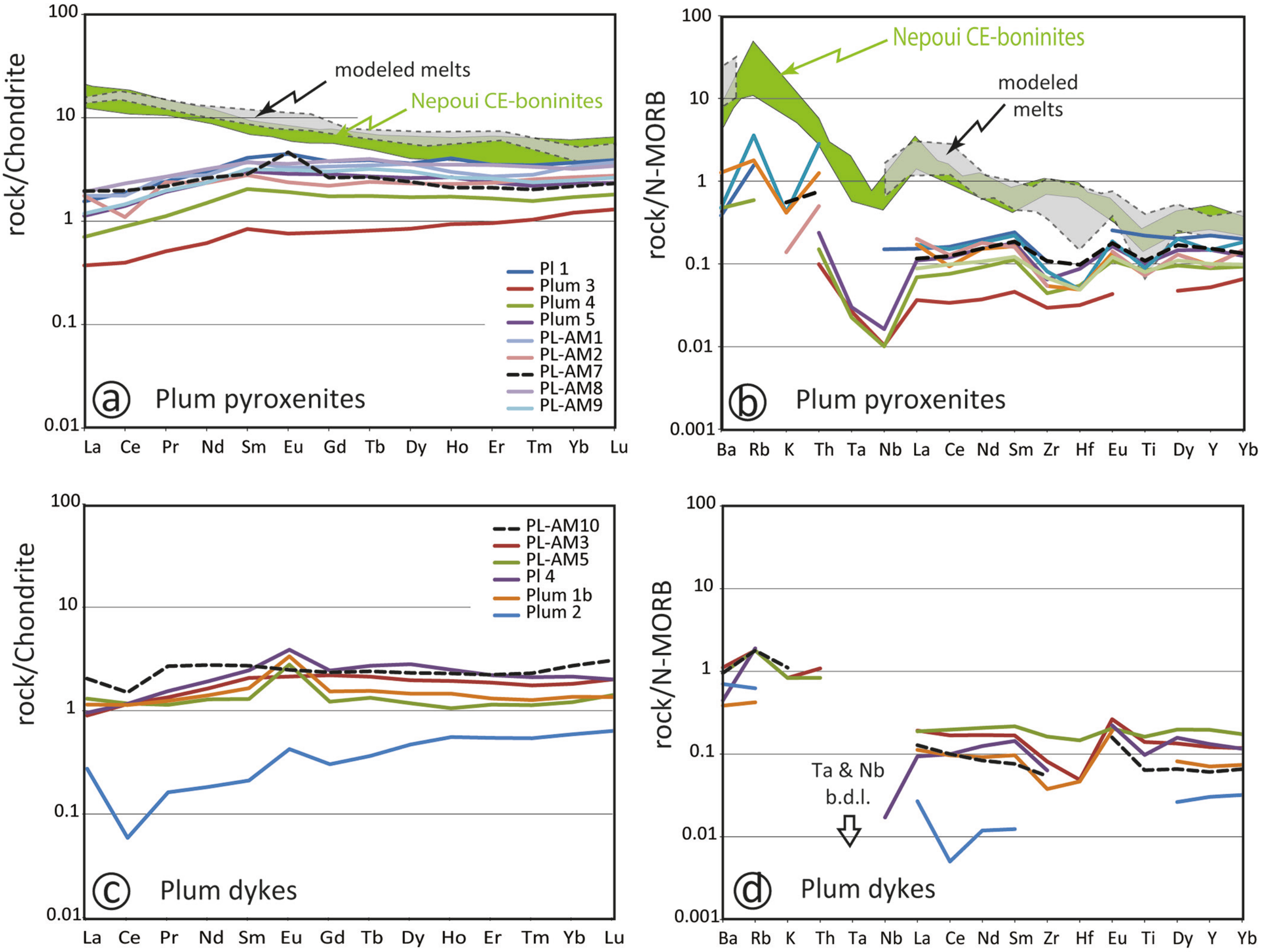

Fig. 10 - a) Chondrite-normalized REE diagram and b) REE and trace element extended diagrams normalized to the N-MORB for Plum pyroxenite body and comparison of the modeled melts with Nepoui CE-boninites. c) and d) the same diagrams for the associated dikes to show the similarity in composition with the main intrusive body. The dotted patterns represent the dated samples. Data from Cluzel et al. (2024).

1980). Such relative chronology is consistent with decreasing grain size from pyroxenites to basalts, thus suggesting dike emplacement during the cooling of the host peridotite.

Depending on their orientation and location within the high-strain domain, pyroxenite dikelets are generally undeformed, post-dating ductile shear deformation of the peridotite. However, some pyroxenite dikes display ductile shearing or boudinage when parallel to foliation in high strain domains, or ptygmatic folding when perpendicular to it (Titus et al., 2011). Sheared or folded pyroxenite dikes are therefore contemporaneous with the late stages of transcurrent motion. The orientations of hornblende-gabbro dikes cluster around N5°E, N40°E and N130°E, broadly consistent with the orientation of dikes in the rest of the ophiolite (Cluzel et al., 2021), bearing no direct relationship to BTF. Finally, undeformed basalt dikes display straight boundaries and cluster around N30°E (Titus et al., 2011). They were seemingly channelized in already cold foliated rock.

In the Ouassé bay, the pyroxenites occur as 5-15 cm thick dikelets that typically intersect the host peridotite foliation at variable angles. Rare concordant layers of orthopyroxenites occur as well, and some are boudinaged. Pyroxenites mainly consist of amphibole-bearing (Amp ~5-40 vol. %) websterites and minor orthopyroxenites containing ~5 vol. % of olivine or clinopyroxene. Pyroxenite textures are highly variable, ranging from cumulitic to porphyroclastic or granoblastic-polygonal (Ferrari, 2022). Hornblendes from two websterite samples were dated by the $^{40}Ar/^{39}Ar$ method yielding a cooling age of 56.01 ± 0.19 Ma and 56.05 ± 0.17 Ma respectively, without any evidence for partial degassing or excess argon. The dated amphiboles are magnesio-hornblendes chemically analogous to those from the Plum pyroxenite intrusion (Cluzel et al., 2024).

Xu et al. (2021) proposed that the websterites from the Ouassé bay resulted from migration of boninitic melts into the host harzburgite. However, trace element composition of the calculated melts in equilibrium with clinopyroxene are distinctly enriched in incompatible elements with respect to boninitic melts and are similar to high-Mg adakites, thus testifying the involvement of a distinct slab-derived component in the genesis of these pyroxenites (Fig. 11) (Ferrari, 2022). By contrast, the orthopyroxenite-forming liquids have a boninitic affinity.

The two studied pyroxenite occurrences (Plum and Ouassé) partly differ by chemical composition, structure, size and, to some extent, their timing. The geochemistry of these pyroxenites shows that they were likely generated from hydrous melting of moderately depleted harzburgite previously modified by slab melt inputs, similar to the parental magma of the CE-boninite.

The Ouassé samples are measurably older than the Plum samples at the 2s confidence level and they are associated with the HT Bogota shear zone. Here, the emplacement of different types of pyroxenite-forming liquids (boninites and high-Mg adakites) was contemporaneous or closely followed ductile deformation. The age of 56 Ma places the genesis of Ouassé pyroxenites and ductile shearing at the onset of subduction. The apparently younger Plum pyroxenites occurred in much larger bodies and were dominated by more depleted parental magmas, yet they were also associated with large-scale transcurrent tectonics.

Nepoui clinoenstatite-boninite and boninite-series dikes

Boninite outcrops from Plaine des Gaiacs, referred to as Nepoui clinoenstatite (CE)-boninite, have been extensively studied since their discovery (Sameshima et al., 1983). Reassessment of these outcrops has shown that Nepoui CE-boninite consists of blocks enclosed within the serpentinite sole of Peridotite Nappe together with other dismembered magmatic rocks (Cluzel et al., 2016). The Nepoui boninite displays hyaloporphyritic texture with some 50-60% dark glassy groundmass including poly-synthetically twinned clinoenstatite, orthopyroxene (bronzite) and olivine microphenocrysts, and accessory clinopyroxene, hornblende and chromite. Clinoenstatite laths, a diagnostic component of boninites, 1-4 mm long, contain minute chromite grains and appear as decussate aggregates.

The Nepoui boninites have andesitic major elements composition (SiO_2 = 55.5 wt.%, Al_2O_3 = 10.0 wt.% on av. for 10 samples) with low CaO (3.8 wt.% on av.) and FeO contents (7.6 wt.%), low CaO/Al_2O_3 ratio (0.4 on av.), very low K_2O (0.6 wt.%) and TiO_2 (0.2 wt%). In contrast, they display high MgO (11-15 wt.%) and high contents in compatible elements (Cr = 486-1371 ppm, Ni = 190-1640 ppm) (Cluzel et al., 2016). In contrast with the classical U-shaped REE pattern

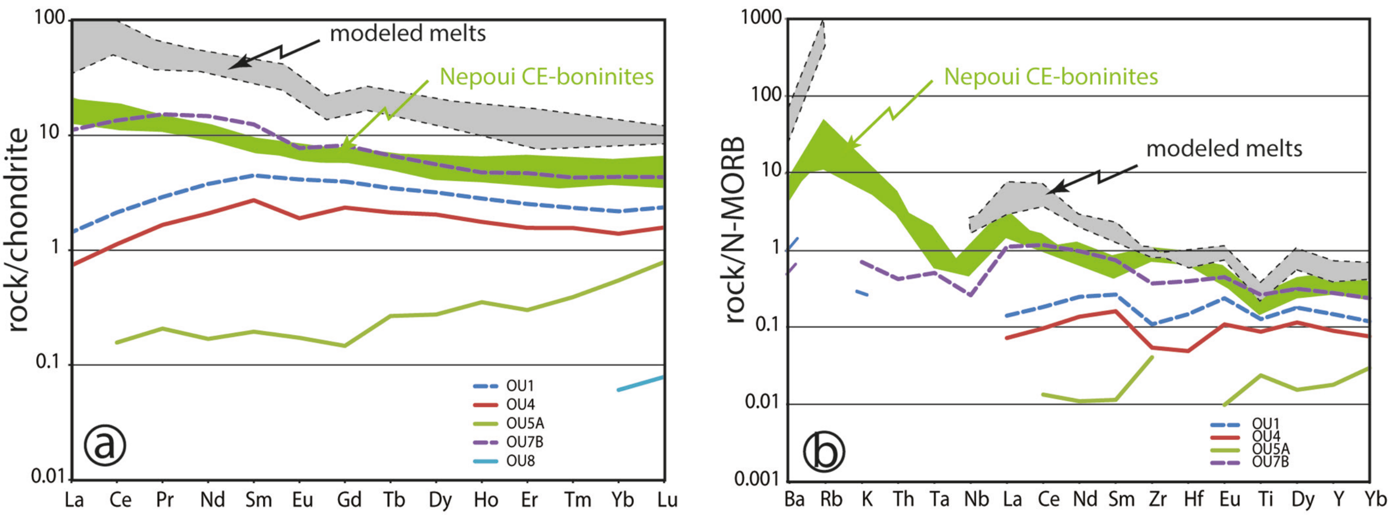

Fig. 11 - a) Chondrite-normalized REE patterns and b) extended REE and trace elements patterns for Ouassé pyroxenite dikelets to show the large difference between the modeled melts and Nepoui CE-boninite. Data from Cluzel et al. (2024) and Ferrari (2022).

of boninites of the type locality (Bonin islands; Crawford et al., 1989; Shervais et al., 2021), Nepoui CE-boninites display slightly concave “spoon-shaped” REE patterns with significant LREE enrichment ((La/Sm)N=2.2), which are similar to those of the less REE-depleted boninites from Cape Vogel (Walker and Cameron, 1983; König et al., 2010; Kamenetsky et al., 2002; Cluzel et al., 2016) (Fig. 4Sa). According to the classification scheme of Pearce and Reagan (2019), they plot in the domain of high-silica boninites. On the expanded incompatible trace elements diagram normalized to N-MORB, they exhibit a well-defined negative anomaly in Nb, Ta and Ti and a positive anomaly in Zr and Hf, very similar to the patterns of Cape Vogel boninites (Fig. 4Sb).

Based on multi-element geochemical modeling, Cluzel et al. (2016) proposed that Nepoui CE-boninites derived from a moderately depleted peridotite that reacted with low degree partial melts from a slab source similar to the amphibolites of the metamorphic sole. Remarkably, the calculated melting residue strongly differs from the ultra-depleted harzburgites of Peridotite Nappe, ruling out that these harzburgites represent the mantle residue left after boninite extraction. $^{40}Ar/^{39}Ar$ dating of glassy fragments yielded Early Eocene cooling ages (47.4 ± 0.9 Ma and 50.4 ± 1.3 Ma) (Cluzel et al., 2016). Considering the glassy character of the rock and possible argon loss, the older age is likely to approach the emplacement age. Numerous dikes within the Peridotite Nappe show geochemical features akin to those of the Nepoui CE-boninites, i.e., similar REE contents, high-MgO, negative Nb, Ta and Ti anomalies, positive Zr and Hf anomalies (Fig. 4Sc, d), and were referred to as boninite-series by Cluzel et al. (2016). However, none of them are sensu stricto boninites and they dominantly plot in the domain of high-Mg andesites on the classification diagram of Pearce and Reagan (2019). Although no modeling was performed for these rocks, a process similar to that of CE-boninites may be postulated for their origin; i.e., slab melting or partial melting of a mantle source modified by slab melts (e.g., Wood and Turner, 2009). U-Pb zircon dating of these rocks provided a narrow age range between 54.5±0.7 Ma and 53.2±0.6 Ma (Cluzel et al. 2016), within the age range of the other dikes of the Peridotite Nappe.

Hornblende-bearing dikes and hornblendites

Hornblende-gabbro and diorite dikes are common in ophiolites from various tectonic settings. In New Caledonia, they occur at all levels of the ophiolite but decrease in frequency from the base to the top of the Peridotite Nappe. Their compositions vary from hornblendite (with less than 5% plagioclase) to leucocratic anorthosite (less than 5% hornblende) through hornblende gabbro/diorite (Fig. 5Sa). Many hornblende-bearing dikes display structures that record high- to medium-temperature deformation compatible with transcurrent kinematics (Cluzel et al., 2021, 2024). Hornblendite samples display slight LREE depletion with hook-shaped patterns typical of amphibole-dominated modal compositions (Fig. 5Sb) (Henderson, 1984). The chemistry of hornblende-gabbro/diorite dikes shows higher incompatible elements abundances compared to hornblendites, with positive and negative Eu anomalies, systematic negative Nb, Ta and Ti anomalies, and Zr-Hf positive anomalies (Fig. 5Sd). Variable depletion in high-field strength elements (HFSE) in many hornblendites and hornblende gabbro/diorite samples suggests the occurrence of residual garnet in their sources. U-Pb dating of zircons from 12 samples provides crystallization ages from 55.7±1.3 Ma to 52.3±0.9 Ma with an average of ca. 54 Ma (Cluzel et al., 2006, 2024).

Anorthosite dikes

Light-colored rocks sharply contrasting in the field with the host peridotite form cm- to m-thick coarse to medium-grained dikes that represent the leucocratic (amphibole-poor) endmember of the hydrous rock suite. They typically show variable REE contents with flat or slightly U-shaped patterns, some of which are very depleted, and most show a prominent Eu positive anomaly that suggests plagioclase accumulation (Fig. 6Sa). They show prominent enrichment in mobile elements and negative Nb anomaly without Ta anomaly; some but not all show a positive Zr-Hf anomaly (Fig. 6Sb). Plagioclase, and in counterpart, hornblende enrichment likely results from solid-state mineral segregation within crystal mushes. The occurrence of compositional layering, hornblendite and anorthosite enclaves within the same gabbro dike is evidence of their cogenetic character (Cluzel et al., 2024). Due to the low Zr content (2-100 ppm) zircons are rare in these rocks; however, one sample with Zr>60 ppm yielded an U-Pb age of 52.6±0.4 Ma ; i.e., within the age range of the bulk of lower Eocene dikes.

Granite dikes

Biotite and quartz-bearing felsic dikes are not uncommon in the Peridotite Nappe and similarly to other dike types display various textures, from granular to pegmatitic, due to relatively slow cooling. They typically contain 71-78.7 wt% SiO_2, 12.3-15.3 wt% Al_2O_3, 3.7-6.7 wt% Na_2O+K_2O, low K_2O (0.1-2 wt%) and low FeO and MgO contents. On the REE diagram normalized to the chondrite C1 (Evensen et al., 1978) two kinds of patterns are distinguished: type 1) spoon-shaped patterns, and type 2) slightly U-shaped patterns (Fig. 7Sa). The type 1 samples display an extreme depletion in HREE and a prominent Eu positive anomaly. On the REE and trace elements diagram normalized to N-MORB, the type 1 granites display variable Nb-Ta negative anomalies and Zr-Hf positive anomalies (Fig. 7Sb).

Type 1 granites display trace-elements patterns typical of adakite series and their similarities with hornblende-bearing dikes likely denote a similar origin, possibly through a lower melting degree and/or fractionation. In contrast, the U-shaped REE patterns of type 2 granites strongly recall that of boninite series rocks, although they are not boninites sensu stricto. Similarly to the other dikes, their U-Pb zircon ages define a narrow range between 54.2 Ma and 53.1 Ma (Cluzel et al., 2024).

Dolerite dikes

Dolerite dikes 1-10 m thick are relatively rare in the Peridotite Nappe, and a crosscutting relationship with other dikes was never observed; however, microcrystalline texture and occurrence of chilled margins suggest intrusion in an already cold peridotite and late emplacement compared to other dike types. Dolerite dikes are oriented N20°E on average (Titus et al., 2011; Cluzel et al., 2021), suggesting brittle NW-SE-directed extension at the time of dolerite intrusion.

The dolerite dikes have basalt or basaltic andesite compositions and show LREE depletion similar to N-MORB (Fig. 8Sa). They also have variable but prominent negative anomalies in Nb and Ta and weakly negative Ti anomalies (Fig. 8Sb). These characteristics allow a classification as island arc tholeiites (IAT). A K-Ar age of 50 Ma was previously reported for a dolerite crosscutting a gabbronorite cumulate lens at Montagne des Sources (Massif du Sud) (Paris, 1981). One IAT dolerite dike from the Boulinda Massif (west coast) yielded a $^{40}Ar/^{39}Ar$ cooling age of 50.4±0.2 Ma (Cluzel et al., 2021).

Summary and geodynamic implications

The geochemistry of the pyroxenite dikes shows that they were likely generated from hydrous melting of moderately depleted harzburgite previously modified by slab melt inputs, similar to the parental magma of the CE-boninite. The local New Caledonia harzburgites are too depleted to be the melting residue of these melts (Cluzel et al., 2016; Secchiari et al, 2022b) indicating a different mantle source.

The diversity of dikes generated during subduction initiation in the New Caledonia ophiolite reveals a complex interplay of melt sources and petrogenetic processes including:

- slab-derived melts produced by low-degree partial melting of high-temperature amphibolites (hornblende gabbro-diorite series), variably interacting with an ultramafic component.
- boninite-like melts (CE-type) derived from depleted mantle wedge peridotites metasomatized by slab melts.
- hydrous mantle melts generated by partial melting of mantle wedge peridotites previously modified by CE-boninitic melts, forming hornblende-pyroxenites and websterites.
- tholeiitic (IAT) melts sourced from relatively fertile mantle domains and emplaced into an already cooled lithosphere as doleritic dikes.

The volumetrically predominant hornblende-gabbro/diorite dikes are likely to have been mostly slab-sourced and were intruded during the whole episode of forearc magmatism (55.5 Ma to 50 Ma). The end of this episode of slab melting that recorded slab cooling at ~50 Ma coincided with the occurrence of mantle-sourced IAT dolerites. Therefore, the ophiolite of New Caledonia belongs to a minor group of supra-subduction ophiolites in which the magmatic activity is dominated by adakite-like rocks that resulted from partial melting of the subducting slab (Furnes and Dilek, 2017). Melts generated during the early stages of subduction east of New Caledonia record a complex and short-lived magmatic evolution, dominated by slab-derived components. At the onset of subduction, the system was characterized by high-temperature conditions, and the earliest melts were produced before significant sediment input into the subduction zone. Magmatic rocks that erupted or intruded in the forearc soon after subduction inception in the interval 56-50 Ma generally do not display any discernable evolution through time except an increase of the Th/Ta ratio and negative Nb (and Ta) anomaly, which possibly record an increasing influence of amphibole (i.e., hydration) in the source rock.

Geochronological and geochemical data indicate that melting occurred over a relatively brief time interval but involved multiple sources, with a predominance of slab melts. This diversity is comparable to observations from other subduction systems, such as SW Japan (Kimura et al., 2014), where forearc magma variability is attributed to interactions between slab-derived melts and heterogeneous mantle sources. Similar conclusions have been drawn for the West Philippine ophiolites (Yu et al., 2020), where early magmatic products range from normal to enriched MORB-like compositions without significant boninite production. These observations challenge the so-called "subduction initiation rule" (SIR; Whattam and Stern, 2011), which is largely based on the Izu-Bonin-Mariana (IBM) system and predicts a characteristic sequence of forearc basalts followed by boninites prior to arc magmatism. Likewise, the magmatic evolution of the New Caledonia ophiolite does not conform to the classical supra-subduction ophiolite sequence (N-MORB → IAT → boninite) described by Dilek and Furnes (2011).

The discrepancy between the New Caledonia and IBM systems reflects fundamentally different subduction initiation mechanisms. In the IBM case, subduction began within an old, cold oceanic plate, promoting the early generation of forearc basalts. In contrast, subduction in New Caledonia initiated in proximity to a spreading center and involved young, hot, and buoyant oceanic lithosphere (Cluzel et al., 2012, 2020). Under such conditions, the thermal structure of the slab and mantle wedge was not conducive to the formation of typical forearc basalts at the earliest stages.

Tholeiitic (island arc tholeiite, IAT) basalt dikes were emplaced several million years after subduction initiation, once the downgoing plate had cooled sufficiently to stabilize eclogite. The resulting increase in slab density likely induced slab steepening and possibly the onset of slab retreat. This, in turn, would have facilitated asthenospheric upwelling and partial melting in the mantle wedge, leading to IAT magmatism. Subsequently, magmatic activity appears to have migrated away from the forearc toward the developing volcanic arc (the Loyalty Arc), marking the cessation of significant melt generation in the forearc domain.

MODERATE TO LOW-TEMPERATURE PROCESSES

Solid phase transfer into ophiolitic mantle: evidence from New Caledonia and global analogues

Occurrences of zircon, rutile and titanite within mantle harzburgites and podiform chromitites provide sensitive records of crust-mantle interaction in supra-subduction settings. Although metasomatic addition via fluids and melts has long been assumed to explain these phases, recent studies have demonstrated that mechanical entrainment of solid mineral grains represents a fundamental and previously under-recognized mechanism. The Peridotite Nappe of New Caledonia offers one of the clearest examples of this process. Thus, it forms the basis for a revised model of crustal material transfer into the forearc mantle.

Evidence for Solid-Phase Transfer in New Caledonia

Aitchison et al. (2022) established that rutile and zircon hosted in unserpentinized forearc harzburgites and chromitites of the New Caledonian Peridotite Nappe include populations of inherited xenocrysts with U-Pb ages much older than the Eocene subduction event.

The xenocrystic zircon and rutile display Proterozoic to early Phanerozoic ages with a predominant population of Albian zircons (c. 100 Ma) (Fig. 12) that correspond to detrital age provinces of sedimentary rocks in the downgoing slab rather than any source within the overlying mantle wedge. Their rounded morphologies, lack of reaction coronas, and inclusion within chromite support a model in which grains were transferred mechanically, rather than precipitated from melts. Preservation of rutile U-Pb systematics indicates transfer and residence at temperatures below ca. 600-650 °C. These grains were likely liberated from metamorphosed slab materials beneath an Eocene forearc at depths of ~40-60 km. They were subsequently transported into the overlying mantle via the subduction channel.

Building on this foundation, Patias et al. (2024) combined zircon U-Pb-Hf isotope data with TiO_2 polymorph geochemistry for mantle peridotites and the Tiébaghi chromitites. They demonstrated the coexistence of (i) inherited zircon

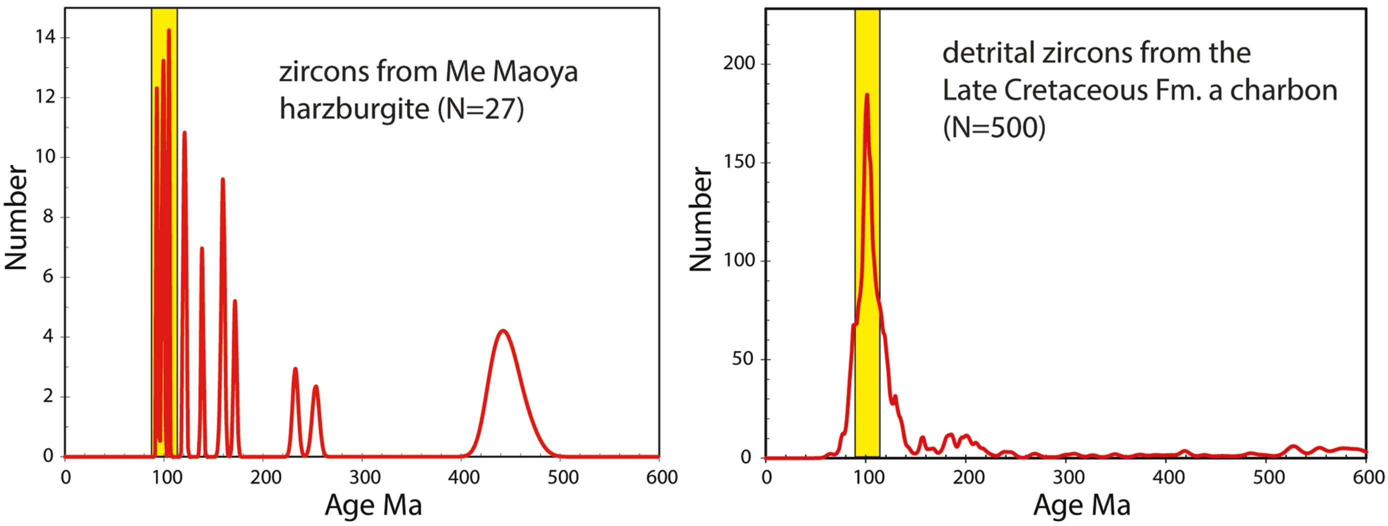

Fig. 12 - Age comparison of zircons extracted from the Me Maoya harzburgite (a) and detrital zircon population of subducted Late Cretaceous sediments (b) with emphasis on the predominant Albian (c. 100 Ma) zircon population. Data from Aitchison et al. (2022).

and rutile xenocrysts, mechanically introduced from the slab, and (ii) Eocene magmatic zircon and rutile that constrain the timing of forearc melt activity and chromitite formation. Together with the petrographic evidence, these data document a multistage "genealogy" for accessory minerals in the Peridotite Nappe.

Accessory minerals in ophiolitic mantle as a global phenomenon

The New Caledonian example forms part of a growing global dataset showing that xenocrystic zircon and rutile are common components of mantle sections in supra-subduction ophiolites. Chromitites and mantle peridotites from the Tethyan Luobusa and Dongqiao ophiolites (Tibet) contain zircon, rutile, kyanite, corundum, coesite, diamond and moissanite with age spectra ranging from Archean to Mesozoic (e.g., Bai et al., 1993; Griffin et al., 2016; McGowan et al., 2015; Yamamoto et al., 2013; Yang et al., 2014, 2021). The Kermanshah ophiolite, part of the Zagros suture in Iran, contains mantle peridotites and chromitites with inherited zircon populations. Moghadam et al. (2022) demonstrated that zircons in the Neyriz-Kermanshah mantle section include Neoproterozoic-Paleozoic xenocrysts, interpreted as transported crustal material from the northern margin of Gondwana recycled into the supra-subduction mantle during Neotethyan subduction. Other Tethyan ophiolites in Albania, Greece and Turkey (e.g., Mirdita, Pindos, Vourinos, Aladag) contain recycled zircon-rutile assemblages reflecting continental material introduced into the mantle wedge (Fu et al., 2015; Kapsiotis et al., 2016; Lian et al., 2018, 2020; Xiong et al., 2017). Similarly, Cuban ophiolites host xenocrystic zircon, rutile and monazite with age signatures compatible with distal continental terranes (Proenza et al., 2018; Rojas-Agramonte et al., 2016). These global occurrences show consistent patterns with accessory minerals within peridotites and chromitites commonly preserving inherited age spectra incompatible with in-situ mantle processes.

Taken together, observations from New Caledonia, supported by those from other global ophiolite belts, confirm that solid-phase transfer of zircon, rutile, titanite and related minerals is a widespread process during early subduction. Grains liberated from metasedimentary and metabasic rocks in the downgoing plate are mechanically entrained within the subduction channel, transferred into the forearc mantle wedge, and preserved through encapsulation in chromitite and refractory harzburgite. These accessory minerals record both the provenance of recycled crustal components and the timing of melt focusing, chromite saturation and forearc magmatism. The New Caledonian ophiolite also contains rare diamond and moissanite xenocrysts (Aitchison et al. 2025) with a light carbon isotope composition similar to that in Tethyan examples cited above. Work on these unusual mineral occurrences is on-going in an attempt to understand the complexities of mineral genesis. The New Caledonia Peridotite Nappe, therefore, represents a key natural laboratory for understanding the role of solid-state transfer in the petrogenesis and metallogeny of supra-subduction mantle.

Serpentinization in the New Caledonia Ophiolite

The extensively serpentinized New Caledonia Peridotite Nappe offers a rare opportunity to examine processes of mantle-fluid interaction from oceanic spreading and subduction initiation to forearc evolution and late-stage exhumation. Over recent decades, serpentinization within the New Caledonia ophiolite has received increasing attention, with a series of studies collectively outlining a multi-scale, polyphase serpentinization history spanning from the Late Cretaceous to the Quaternary.

Orloff (1968) provided the earliest assessment of serpentinization in the New Caledonia ophiolite, documenting a systematic decrease in the degree of serpentinization from the base to the top of the peridotite massifs. Subsequent studies by Gautier et al. (2016) and Quesnel et al. (2016) examined serpentine-bearing fault zones, characterizing their kinematics and clarifying the mechanisms of ophiolite emplacement onto the continental basement. These studies identified three distinct structural levels corresponding to variations in serpentinization degree and the development of specific syn-deformation serpentine assemblages. They emphasized the key role of the serpentinite sole, which comprises massive tectonic breccias overlying a mylonitic serpentinite layer, in localizing strain during ophiolite emplacement over the continental margin.

Other studies have used New Caledonian serpentinized peridotites as a case study to reconstruct the evolution and redox conditions during progressive serpentinization (Frost et al., 2013), as well as the fluid-rock interactions involved (Mothersole et al., 2017). These studies have also evaluated the reliability of ophiolitic serpentinites as analogues for abyssal seafloor serpentinization and subduction fluxes. Frost et al. (2013) reconstructed the sequence of serpentinization and the physicochemical conditions in New Caledonian dunites. These authors distinguished three generations of serpentine veins and also showed how increasing fluid involvement and magnetite formation progressively sequestered Fe from early serpentine-brucite assemblages. Their results demonstrate a shift from rock-dominated to fluid-dominated serpentinization. Magnetite growth drove higher XMg in later serpentine generations and released H_2. Comparisons between New Caledonia and abyssal serpentinites (Mothersole et al., 2017) reveal that although the reaction sequences and serpentine polymorphs are similar, New Caledonia serpentinites generally have lower concentrations of Cl, S, and C and more reduced Fe than their oceanic counterparts. These differences reflect different fluid sources (i.e., slab- versus seawater-derived) and varying degrees of post-serpentinization weathering. This indicates that New Caledonia serpentinites primarily document subduction-related hydration rather than seafloor alteration.

Through a comprehensive petro-geochemical study, Ulrich et al. (2020) determined the paragenetic sequence of serpentinization in New Caledonia to be lizardite-1 → lizardite-2 → antigorite → chrysotile → polygonal serpentine. Lizardite accounts for approximately 80% of the total serpentine. Trace-element systematics indicate that the transition from primary peridotite minerals to lizardite-1 was nearly isochemical. Later serpentine generations, however, record open-system behavior marked by progressive Fe depletion, increasing Fe^{3+}/Fe_{tot} ratios, and systematic enrichment in fluid-mobile elements (Cs, Rb, Ba, U, and LREE), coupled with strong Ce negative and U positive anomalies (Fig. 13).

Monte Carlo modeling of $\delta^{18}O$-δD compositions shows that the main serpentinization fluids came from the dehydration of altered oceanic crust (AOC) during the initial stages of subduction, at temperatures between 250 and 350°C, with possible contributions from fluids derived from sediment and/or serpentine from the descending plate (Fig. 14).

Building on this framework, Raia et al. (2022) investigated serpentinites exposed within the HP-LT metamorphic complex of northwestern New Caledonia and identified two distinct groups. One group displayed trace-element and isotopic signatures indistinguishable from those of the overlying New Caledonia Ophiolite (Ulrich et al., 2020) and was interpreted as mantle-wedge derived. The second group had elevated $\delta^{18}O$ values and was interpreted as an exhumed portion of the downgoing plate. This dual provenance makes New Caledonia one of the few known examples that preserves both slab-derived and mantle-wedge serpentinites within the same subduction complex.

AOC-derived fluids were not the only contributors to serpentinization. Ulrich et al. (2020) proposed the existence of a low-temperature (~100°C) meteoric component to explain the formation of the youngest serpentine generation that comprises the serpentinite sole. Corre et al. (2023) confirmed this hypothesis by documenting Quaternary serpentinization events younger than 2 Ma based on (U-Th)/He magnetite ages. These events occurred at temperatures of ~95°C, which is consistent with earlier thermal estimates. These results demonstrate that serpentinization is active at shallow structural levels under present-day conditions through the circulation of hyperalkaline fluids similar to those discharged at Prony Bay. There, emitted gases (H_2, CH_4, and N_2) show a linear H_2-CH_4 relationship, which is indicative of low-temperature methanogenesis during serpentinization (Barnes et al., 1978; Deville and Prinzhofer, 2016; Monnin et al., 2014; Pisapia et al., 2017; Corre et al., 2023).

Corre et al. (2023) documented natural carbonation occurring simultaneously with Quaternary serpentinization. They demonstrated that, at relatively high temperatures (~95°C), reactions between olivine, (Mg,Fe)-serpentine, and CO_2-rich fluids produce a distinctive mixture of dolomite, Fe-poor serpentine, magnetite, Fe-brucite, and H_2. The major carbonation event affecting New Caledonian serpentinites mainly developed at the base of the ophiolite (in the serpentinite sole) and has been extensively examined in terms of mineralogy (Ulrich et al., 2014) and stable oxygen-carbon (O-C) isotope compositions (Quesnel et al., 2016a, 2013). These studies demonstrated the meteoric origin of carbonation and its relationship to lateritization at the top of the peridotite nappe. In this context, carbonates are dominated by magnesite and are commonly associated with amorphous silica. Both are interpreted as having formed contemporaneously at substantially lower temperatures (~30°C) than the dolomite identified by Corre et al. (2023). Based on the synkinematic character of magnesite veins, Quesnel et al. (2013) proposed that tectonic activity during laterization enhanced meteoric water infiltration. This promoted Mg-Si removal and drove widespread carbonation and silicification along the serpentinite sole. Carbonation developed in two main modes: (1) a per descensum process forming magnesite-silica veins concentrated in fractures and (2) pervasive dissolution-precipitation replacing serpentine with magnesite and amorphous silica without obliterating the primary serpentinite textures. The latter is the dominant carbonation mechanism.

Overall, evidence from mineralogy, microstructures, isotopes, tectonics, and fluid chemistry confirms that serpentinization in the New Caledonia ophiolite is polyphasic, long-lived, and spatially heterogeneous. Early AOC (slab)-derived fluids hydrated the mantle wedge during the initiation of subduction, while later meteoric fluid circulation during and after obduction generated low-temperature serpentinization, magnetite formation, and H_2/CH_4 production. These processes continue today and generate hydrogen seepage. These meteoric fluids also induced pervasive carbonation and associated silicification along the serpentinite sole.

Slab-derived melts and fluids at the origin of antigorite-tremolite veins

The harzburgites, lherzolites and dunites of the Peridotite Nappe of New Caledonia are crosscut by joints, through which the rocks have been pervasively serpentinized at relatively low temperature, producing lizardite, brucite, magnetite and minor chrysotile in a near-static environment (see previous section). In a next step, already serpentinized joints were re-opened to produce tension and shear cracks sealed by higher temperature synkinematic fibrous minerals. Most veins only contain fibrous antigorite but some display tremolite-antigorite intergrowths or even pure tremolite. Locally, tremolite-bearing veins and pockets, which do not display evidence for void infill, were generated by metasomatic replacement of the wall rock peridotite. The veins yield high contents of Ca and incompatible elements, which contrast

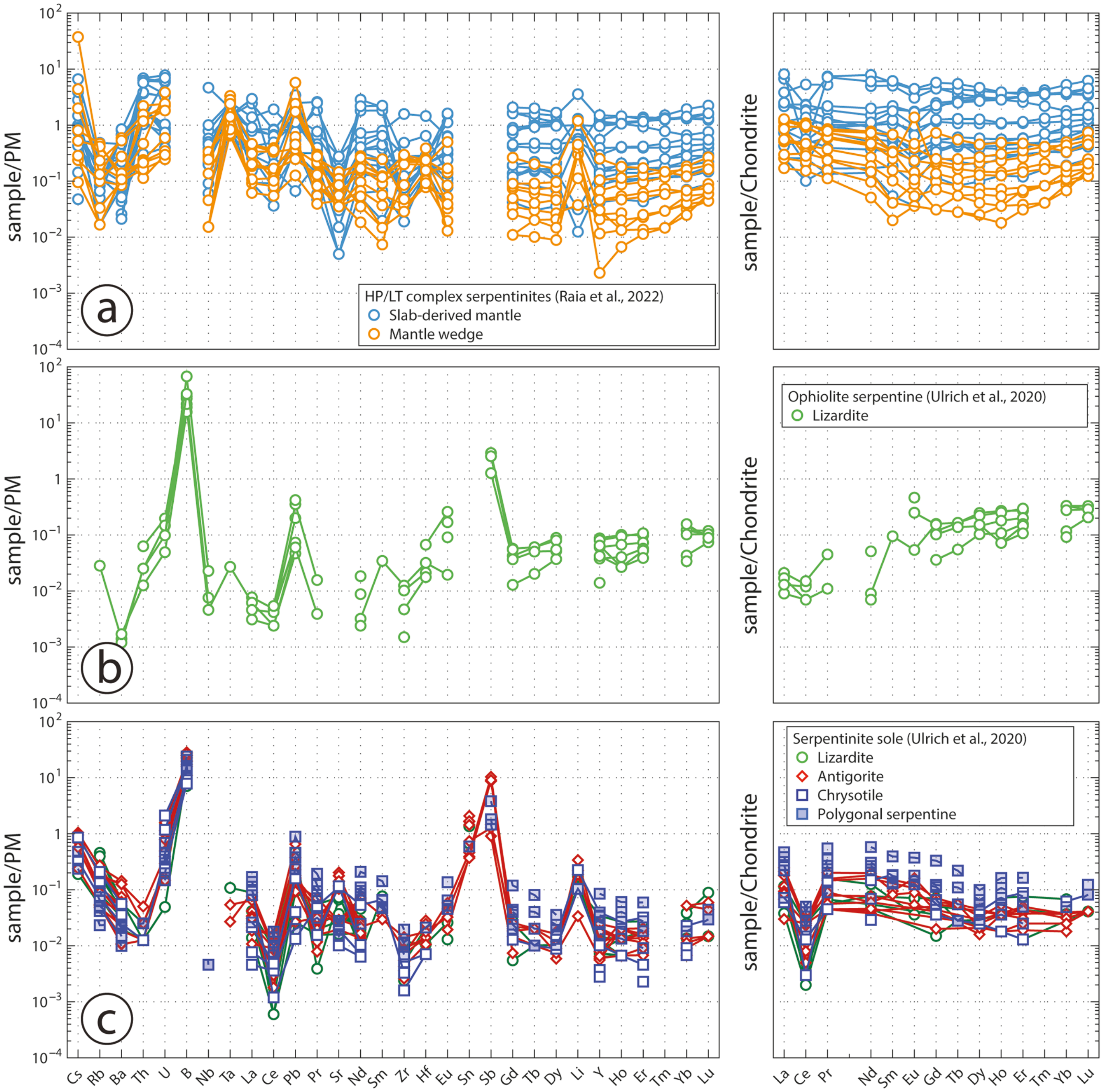

Fig. 13 - Extended trace element (PM-normalized, left) and REE (Chondrite-normalized, right) patterns of HP/LT serpentinites (a) (Raia et al., 2022), and serpentine species from the Peridotite Nappe (b) and the serpentinite sole (c) Ulrich et al., 2020).

with the overall depletion of the peridotite host rock and suggest contribution of an external source. These characteristics raise questions about temperature increase and the influx of calcium (Cluzel et al., 2019).

In general, fibrous crack seals are nucleated on wall rock and the nature of minerals that fill the progressively opening spaces depends strongly on the composition of the host rock. There is a consensus on the fact that synkinematic minerals, which form the crack seals, come from pressure or shear solution and are in equilibrium with pore fluids. Thus, synkinematic mineral growth is at least partly fed by dissolved elements that were carried over short distances (e.g., Baghat and Marshak 1990; Beach 1974, 1977; Bons and Jessell 1997; Durney 1972, 1976; Pollard and Segall 1987; Rutter 1983). Accordingly, only serpentine minerals (antigorite, lizardite, chrysotile, polygonal serpentine, depending upon P-T conditions) are expected to be in equilibrium with the more or less deeply serpentinized peridotite wall rock (Andreani et al. 2007; Kurat et al. 1993).

Ultramafic rocks of the Peridotite Nappe contain up to ~ 0.7 wt.% CaO in harzburgites and ~ 2.5 wt.% CaO in lherzolites, yet fractures filled with tremolite, a calcium-rich amphibole, are widespread except within unserpentinized nuclei. The input of calcium can hardly be attributed to mobilization from the peridotite itself; therefore, an external source is needed without taking into account the rise in temperature.

Tremolite crystallization may result from the interaction of serpentinite with Ca-rich metasediments in mélanges (e.g.,nephrite jade; Adams et al., 2007; Adams and Beck, 2009), with mafic rocks in subduction zones (Marocchi et al., 2010; Laborda-López et al., 2020), from the recrystallization of dikes that crosscut serpentinites (e.g., rodingites; Bach and Klein, 2009; Harlow and Sorensen, 2005; Koutsovitis et al., 2013; Sivell and Waterhouse, 1986), from the mobilization of Ca from pyroxenes during serpentinization (Python et al., 2011), or from the "hydrothermal" mobilization of Ca from calcite veins originating from seawater at shallow depths (Agrinier et al., 1996). In New Caledonia, tremolite also appears locally in greenschist-facies mylonitic gabbronorite cumulates (Ouen Island "jade"; Maurizot and Lesimple, 2012). However, in these rocks, tremolite displays a strong preferred orientation, yet never exhibits an asbestiform texture. In contrast, the tremolite occurrences discussed here are always found in cracks in serpentinized peridotite, far from any mafic crustal rock.

The $^{87}Sr/^{86}Sr$ ratio in harzburgites and lherzolites of the Peridotite Nappe, which are the most common wall rocks of antigorite and tremolite-bearing veins, covers a relatively large range (0.7049-0.7077) (Secchiari 2016; Secchiari et al. 2019) and a certain role of "primary" serpentinization may be suspected. However, there is no correlation between the LOI, which represents the degree of primary serpentinization, and the Sr isotope ratio of unserpentinized lherzolites and harzburgites (LOI = 0-0.7wt%; $(^{87}Sr/^{86}Sr)_i$ = 0.7077-0.7054) and moderately serpentinized ones (LOI = 6.0-10.7wt%; $(^{87}Sr/^{86}Sr)_i$ = 0.7075-0.7049) (Secchiari 2016, 2019). A moderate degree of primary serpentinization does not appear to have significantly modified the Sr isotopic composition of the peridotites. Therefore, serpentinization alone cannot account for the radiogenic character and variability of the $^{87}Sr/^{86}Sr$ ratios observed in the New Caledonia peridotites, which are more plausibly attributed to the incorporation of slab-derived components (Secchiari et al., 2019).

As far as shear- or pressure-solution origin is considered, the Sr isotope composition of antigorite would reflect that of the peridotite wall rock, pending some influence of circulating fluids. However, the $^{87}Sr/^{86}Sr$ of antigorite veins is much higher than that of peridotites (up to 0.7117), close to the present ocean water composition and even much higher than that of lower Eocene waters (Fig. 15) (Murthy and Beiser 1968; Elderfield 1986; Veizer 1989; McArthur et al. 2012). These values are slightly lower than that of hemipelagic terrigenous sediments (e.g., McLennan et al. 1990; Hemming et al. 2007) and point to sediment-water mixing/leaching. Thus, the highly radiogenic $^{87}Sr/^{86}Sr$ ratios from antigorite veins reflect some influence of subducted sediments on the fluids released by the slab, which infiltrated the supra-subduction mantle and were involved in antigorite crystallization.

Tremolites from veins and pockets display low and constant $^{87}Sr/^{86}Sr$ (0.7042-0.7045) (Cluzel et al., 2019) that clearly differ from that of lherzolite and harzburgites wall-rock (Fig. 15); thus, a direct origin of Ca by leaching of peridotites is unlikely. Alternatively, tremolite seems to have been in equilibrium with "magmatic" fluids, a feature consistent with $\delta^{18}O$ and δH values (see below), even though a certain influence of ocean-like water cannot be excluded. The "sedimentary" signature of antigorite veins, possibly derived from subduction-related fluids, was probably diluted in tremolite-bearing veins, which contain 100-1000 times more Sr than antigorite. It is unlikely that tremolite formed by direct reaction of felsic magma with serpentinized wall rock because in all observed reaction rims around dikes, anthophyllite and/or Mg-chlorite are formed instead of tremolite. In the frequent absence of direct contact between felsic dikes and tremolite veins or pockets, it may be suggested that tremolite merely formed by reaction between hydrous fluids released by subduction and having leached the still hot felsic dikes and the serpentinized wall rocks of active shears or tension cracks (Cluzel et al., 2019).

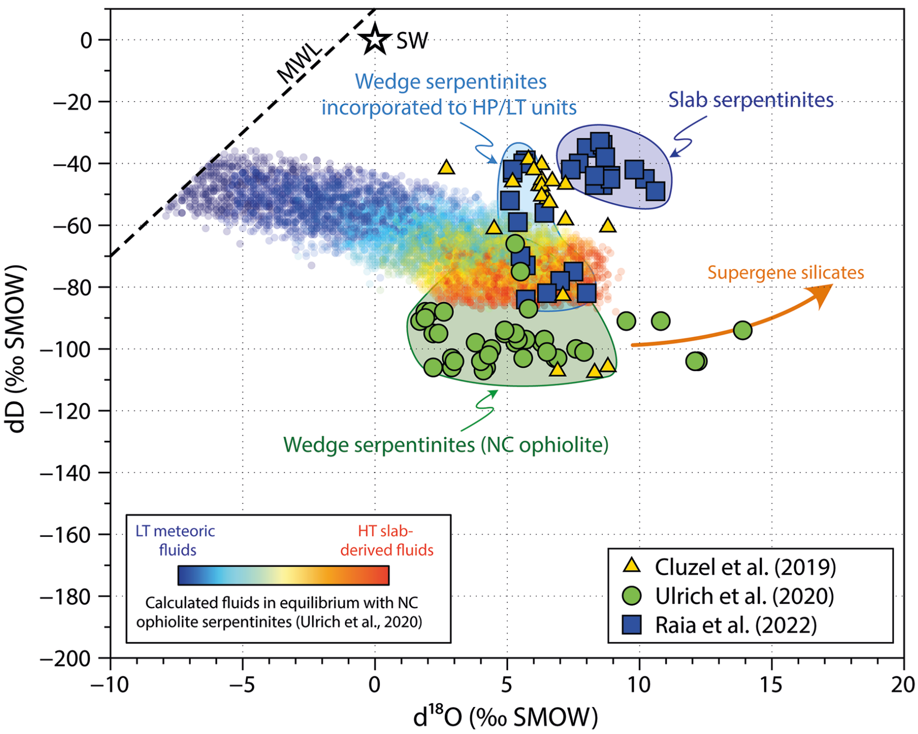

Fig - 14. $\delta^{18}O$-δD compositions of New Caledonia serpentinites composing the Peridotite Nappe (wedge serpentinites; Ulrich et al., 2020) and those from the HP/LT units (Raia et al., 2022). Calculated fluids in equilibrium with wedge serpentinites testify of composite compositions and temperatures that range from HT (~350°C) AOC-derived fluids to LT (<150°C) meteoric waters.

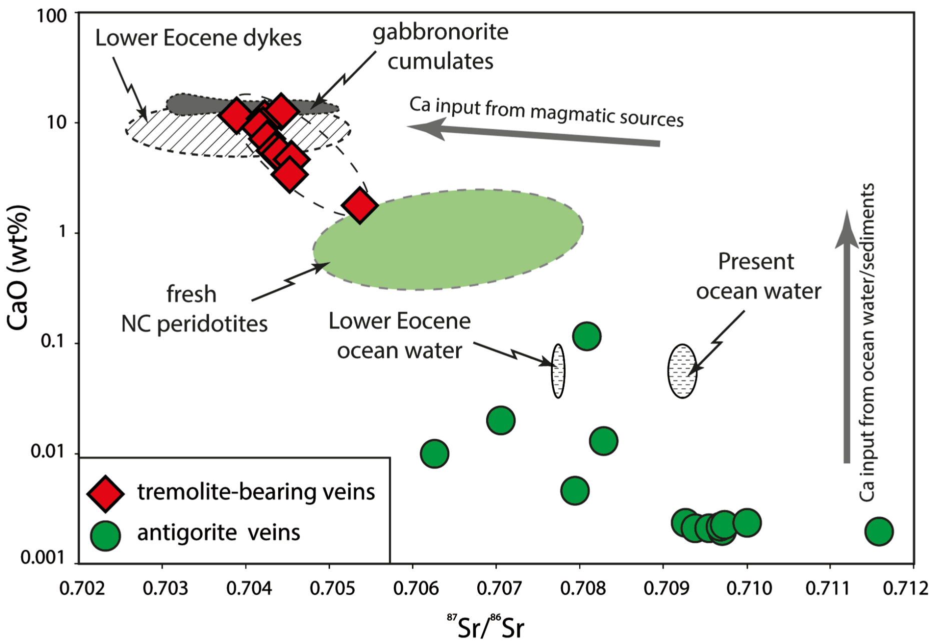

Fig. 15 - Plot of Ca vs. $^{87}Sr/^{86}Sr$ to compare Sr isotopic composition of tremolite and antigorite (Cluzel et al., 2019) to gabbronorites (Secchiari et al., 2016), Early Eocene dikes (Cluzel et al., 2006) from the Peridotite Nappe. Ocean waters compositions are from Murthy and Beiser (1968), Elderfield (1986), Veizer (1989) and McArthur et al. (2012).

The $\delta^{18}O$ and δD of hydrous minerals result from the balance of the isotopic composition of the wall rock, water/rock ratio, mineral-water fractionation coefficients, isotope ratios of circulating water, and temperature. In this study, a probable temperature of tremolite-antigorite formation can be estimated in the range of 300-450°C. Under these temperatures, tremolite and serpentine minerals should display comparable $\delta^{18}O$ values as an equilibrium isotopic fractionation of about $\delta^{18}8O$ Trem-Serp = − 0.3‰ is expected (Zheng 1993). The mean $\delta^{18}O$ values of 6.8‰ and 6.4‰ for tremolite and antigorite, respectively (Fig. 16) (Cluzel et al., 2019), correspond to $\delta^{18}O$ Trem-Serp = + 0.4‰, and are somewhat at variance with the theoretical equilibrium. In fact, in the crystallizing sequence we argue for a slight temperature decrease at the end of tremolite crystallization. All other factors equal, this should imply a small increase of the isotopic fractionation between tremolite and water, and thus an increase in the $\delta^{18}O$ value of tremolite.

The fact that tremolite is actually slightly enriched ($\delta^{18}O$ = 6.8‰) in ^{18}O relative to antigorite ($\delta^{18}O$ = 6.4‰) is consistent with a small temperature decrease. At first order, both minerals likely crystallized in equilibrium with a single aqueous reservoir. Assuming that fluid was in excess at the time of vein formation (i.e., the fluid/rock ratio is isotopically infinite), the $\delta^{18}O$ value of the invading fluid can be estimated between 6.5‰ and 8.5‰ (using the fractionation factors between H_2O and antigorite between 300 and 450°C from Zheng, 1993). These values are consistently expected for the fluids involved in supra-subduction contexts, like the one prevailing for the formation of the studied veins. Indeed, these fluids, originally derived from seawater, underwent significant isotopic exchange with crustal and mantle rocks, as shown by the Sr isotope and REE systematics of vein minerals, which resulted in increasing their initial, low $\delta^{18}O$ value. A magmatic contribution to the fluid budget that would add a high-$\delta^{18}O$ component (about 7‰) to the fluid is permitted by the data. Lizardite formed during the primary serpentinization did not significantly recrystallize when the rock went into the antigorite stability field. Lizardite and antigorite may coexist at low pressure depending upon serpentine composition (e.g., Caruso and Chernosky, 1979; O'Hanley et al. 1989; Schwartz et al. 2013); however, antigorite fibers considered here are nucleated on lizardite "blackwalls" and partly originated from the destabilization of lizardite as shown by the accumulation of iron oxide at the lizardite-antigorite interface. However, the pervasive replacement of "primary" lizardite by antigorite would require an unlikely large water-rock ratio given the relative impermeability of lizardite coatings and restriction of fluid circulation along open fractures.

The formation of tremolite- and antigorite-bearing veins recorded a temperature increase; a heat source is therefore needed as well as a source for Ca. This event was associated with shear/tensile reactivation of pre-existing joints already coated by lizardite. The widespread antigorite-bearing low-Ca veins have highly radiogenic $^{87}Sr/^{86}Sr$ signatures, which testify some influence of subducted sediments. In contrast, this "sedimentary" signature is diluted in high-Ca tremolite, which probably comes from Ca input of direct or indirect magmatic origin. The Sr isotope signature of tremolite, its REE abundances, the $\delta^{18}O$ and δD values, all suggest that the Ca source was the supra-subduction Early Eocene felsic dike system and thus, indirectly, the subducted slab. Europium-positive anomaly and paradoxically high contents of some compatible elements (Cr) suggest that Ca was carried by oxidized hydrothermal fluids that leached the dikes and interacted with Cr-rich wall rock (serpentinized peridotite). These characteristics provide a constraint on the timing of tremolite crystallization, because supra-subduction dikes intruded peridotites within a narrow span of time at ca. 55-50 Ma (U-Pb zircon; Cluzel et al. 2006). Since these dikes mostly crystallized from slab melts and boninite series magmas that formed shortly after subduction inception (Cluzel et al. 2012, 2016), already existing fractures were reactivated in an oblique-extensional regime under relatively high fluid pressure and gave way to magma and laterally/upward to Ca-bearing fluids when the young and buoyant slab had to force its way beneath the nascent fore-arc lithosphere. The heat required for the crystallization of tremolite and antigorite after lizardite was most likely supplied by the injection of supra-subduction slab-derived melts (Cluzel et al., 2019). The coexistence of tremolite and antigorite within the same

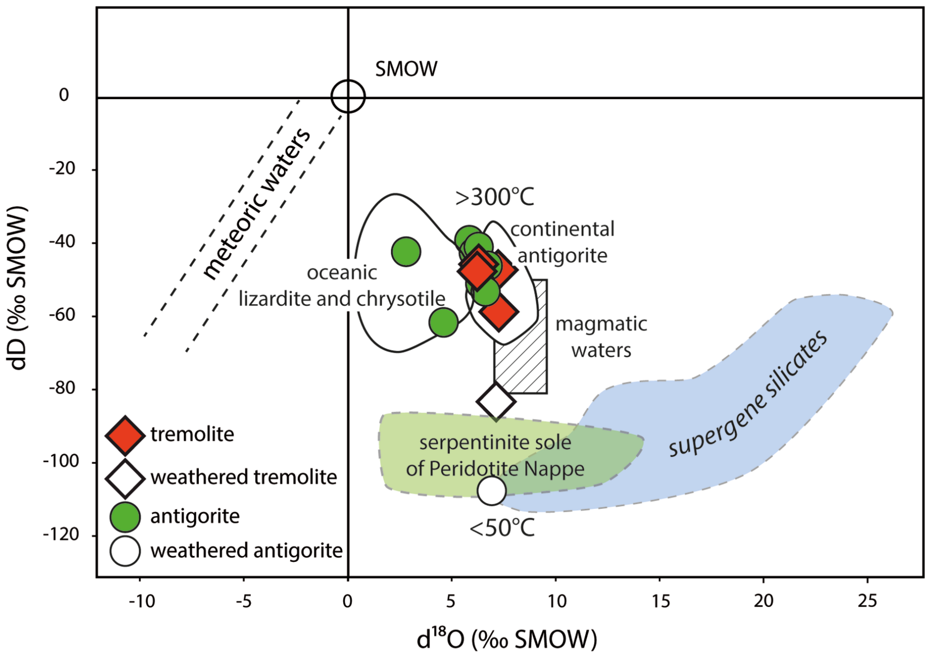

Fig. 16 - $\delta^{18}O$ and δD isotopic ratios of fibrous serpentines and tremolites of the Poro site after Cluzel et al. (2019); "oceanic" serpentinites after Agrinier et al. (1995, 1997); supergene silicates field: "garnierite" after Amisse et al. (2010) and deweylite data after Wenner and Taylor (1974); serpentinite sole of the Peridotite Nappe after Ulrich et al. (2010).

fracture fillings, followed by the crystallization of antigorite alone, may reflect the progressive exhaustion of magmatic fluids, while synkinematic crystallization associated with small-scale faulting and tension cracks continued. This relationship suggests that tremolite-antigorite veins formed during the same tectonic event, with only the fluid composition varying over time. Therefore, irrespective of the upward decrease in primary serpentinization, the development of tremolite-antigorite veins may be related to: (1) static development of low-temperature serpentine minerals along cooling joints, (2) injection of slab-derived supra-subduction magmas and Ca-metasomatic fluids at subduction inception (latest Paleocene), and (3) exhaustion of Ca-metasomatic fluids in a globally cooling mantle wedge (Cluzel et al., 2019).

CONCLUSIONS

The New Caledonia ophiolite provides a comprehensive record of melt, fluid, and solid transfer during the initiation and early evolution of a supra-subduction forearc. Integrated geological, geochemical, isotopic, and geochronological evidence shows that it formed through the superposition of pre-existing mantle domains and short-lived but diverse subduction-related processes.

The harzburgitic main body represents an extremely refractory mantle wedge formed by high degrees of melt extraction, generally beyond clinopyroxene exhaustion. However, U-shaped REE patterns, fluid-mobile element enrichments, Pb anomalies, and radiogenic isotopic signatures indicate later overprinting by slab-derived fluids and minor melts. Isotopic systematics further demonstrate that this Eocene supra-subduction signature was imposed on mantle previously depleted during older melting events. These harzburgites thus represent ancient mantle reworked by hydrous melting and metasomatism. In contrast, the northern lherzolites preserve a moderately depleted abyssal mantle signature, characterized by greater fertility, distinct REE patterns, and different isotopic compositions. These rocks formed in a MOR setting and were later modified by melt infiltration and refertilization, representing pre-forearc mantle fragments incorporated during subduction initiation.

The mantle-crust transition zone (MTZ) and lower crust document the progression from mantle tectonites to magmatic cumulates. The lowermost dunites formed largely by reactive porous flow, involving orthopyroxene dissolution and olivine precipitation within mantle tectonites. Up-section, clinopyroxene- and plagioclase-bearing dunites, wehrlites, pyroxenites, and gabbronorites record increasing melt impregnation and/or cumulate crystallization. Although the balance between replacive and cumulate processes remains debated, all interpretations agree that the MTZ reflects intense interaction between highly depleted mantle and primitive hydrous melts during the earliest construction of the forearc crust. The lower crustal gabbronorites and orthopyroxene-gabbros are crystallization products of primitive, ultra-depleted melt batches derived from refractory mantle sources variably metasomatized by slab-derived fluids. Their extreme REE depletion, combined with enrichments in fluid-mobile elements, indicates that the earliest forearc lower crust in New Caledonia was built not by large, homogenized magma chambers, but by repeated injections of small, chemically distinct melt pulses.

The Lower Eocene dike swarms constitute one of the clearest records of melt diversity during hot subduction initiation. Their age range, between 55.5-50 Ma, closely brackets the earliest stages of subduction and shows that forearc magmatism was both short-lived and compositionally diverse. Several melt types are represented: slab-derived hornblende gabbro-diorite magmas, boninite-like melts, hydrous pyroxenite-forming melts derived from mantle wedge sources modified by slab melts, felsic slab-related melts, and later tholeiitic IAT dolerites derived from more fertile mantle sources. The predominance of slab-derived and slab-influenced melts distinguishes New Caledonia from better-known subduction-initiation systems such as Izu-Bonin-Mariana, where forearc basalts precede boninites. In New Caledonia, subduction began near a spreading ridge and involved young, hot, buoyant lithosphere; consequently, slab melting was favored at the onset, whereas basalt generation was delayed until the slab cooled, densified, and steepened enough to induce asthenospheric upwelling and IAT magmatism (Fig. 17).

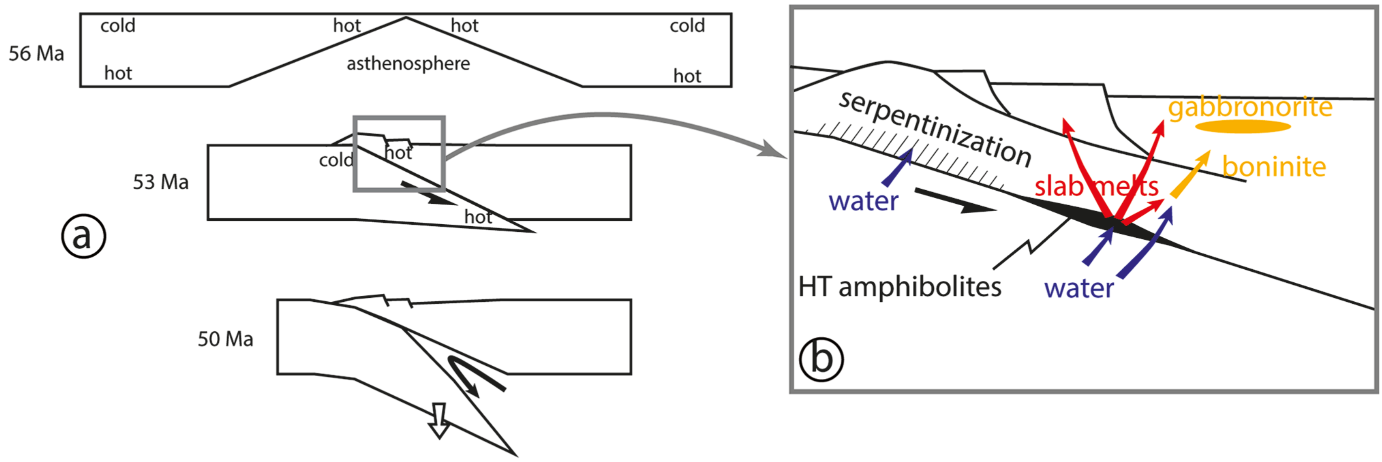

Fig. 17 - (a) Simplified evolution of the Eocene subduction zone, from subduction inception to slab steepening; (b) sketch diagram of fluid and melt circulations in the mantle wedge between 55 and 50 Ma (modified from Cluzel et al., 2024).

Importantly, material transfer from the slab was not limited to fluids and melts. Accessory minerals such as zircon and rutile, with inherited ages, indicate mechanical transfer of solid phases from the downgoing slab into the mantle wedge. A special mention should be made of the formation of diamond and moissanite from C-rich sediments in the subduction zone and their transfer into the mantle wedge, a process seemingly common to many supra-subduction ophiolites. This provides strong evidence for solid-state recycling in supra-subduction environments.

The New Caledonia ophiolite also records prolonged hydration and fluid circulation. The serpentinization of ultramafic rocks was a polyphase process that left only a few serpentine-free nuclei. There is no identifiable trace of pre-subduction serpentinization. Subduction-related serpentinization likely began in relatively cool peridotites (ca. 300 °C) shortly after subduction initiation and has continued to the present day, driven by the circulation of meteoric waters, albeit to a limited extent. These processes led to magnetite formation, hydrogen and methane production, and carbonation, and continue today, as shown by active hyperalkaline springs.

Heat transfer and Ca-Sr metasomatism peripheral to dike emplacement generated metasomatic tremolite pockets and syntectonic tremolite-antigorite veins in already serpentinized peridotites. This event was associated with oblique shallow-dipping subduction. Antigorite-tremolite veins link high- and low-temperature processes, recording infiltration of slab-derived fluids and melts, fracture reactivation, and localized metasomatism during early subduction.

Overall, the New Caledonia ophiolite reveals that forearc lithosphere formed during hot subduction initiation is highly heterogeneous, shaped by multiple interacting processes. This ophiolite stands as a key natural example for understanding material transfer across the slab-mantle interface and the evolution of supra-subduction lithosphere preserved in ophiolites worldwide.

ACKNOWLEDGMENTS

The authors thank Carlotta Ferrando and Tong Liu for their detailed and constructive reviews which did much to improve the manuscript.

ONLINE SUPPLEMENTARY MATERIAL

Supplementary geochemical diagrams associated with this article (Figs. 1S to XS) can be found online at Zenodo.org: https://doi.org/10.5281/zenodo.21626195

Supplementary data to this article are available online at https://doi.org/10.4454/ofioliti.v51i2.584

REFERENCES

Adams C.J., Beck R.J., and Campbell H.J., 2007. Characterisation and origin of New Zealand nephrite jade using its strontium isotopic signature. Lithos, 97: 3-4, 307-322. https://doi.org/10.1016/j.lithos.2007.01.001

Adams C.J., and Beck R.J., 2009. A signature for nephrite jade using its strontium isotopic composition: some Pacific Rim examples. J. Gemm., 31: 153-162. https://doi.org/10.15506/JoG.2009.31.5.153

Agrinier P., Cornen G. and Beslier M.-O., 1996. Mineralogical and oxygen isotopic features of serpentinites recovered from the ocean/continent transition in the Iberia abyssal plain. In: Whitmarsh R.B., Sawyer D.S., Klaus A. and Masson D.G. (Eds) Proc. ODP Sci Res., 149: 541-549. https://doi.org/10.2973/odp.proc.sr.149.223.1996

Aitchison J.C., Clarke G., Meffre S. and Cluzel D., 1995. Eocene arc-continent collision in New Caledonia and implications for regional southwest Pacific tectonic evolution. Geology, 23: 161-164. https://doi.org/10.1130/0091-7613(1995)023<0161:EACCIN>2.3.CO;2

Aitchison J.C., Meffre S. and Cluzel D. 1995b. Cretaceous/Tertiary Radiolarians from New Caledonia. Geol. Soc. New Zealand Miscellaneous Publication 81A, pp. 70.

Aitchison J.C., Cluzel D., Ireland T.R., Zhou R., Lian D., Yan Z. and Yang J., 2022. Solid-phase transfer into the forearc mantle wedge: Rutile and zircon xenocrysts fingerprint subducting sources. Earth Planet. Sci. Lett., 577: 117251. https://doi.org/10.1016/j.epsl.2021.117251

Aitchison J.C., Patias D., Cluzel D., Ireland T.R., Zhou R.J., Lian D.Y., Yan Z. and Yang J.S., 2025. Recycling subducted organic carbon as Diamonds: An example from the New Caledonian forearc ophiolite. Geochem. Geophys.Geosys. 26, 4, e2025GC012250 https://doi.org/10.1029/2025GC012250

Ali J.R., and Aitchison J.C., 2000. Significance of palaeomagnetic data from the oceanic Poya Terrane, New Caledonia, for SW Pacific tectonic models. Earth Planet. Sci. Lett., 177: 153-161. https://doi.org/10.1016/S0012-821X(00)00042-X

Andreani M., Mével C., Boullier A.-M. and Escartín J., 2007. Dynamic control on serpentine crystallization in veins: constraints on hydration processes in oceanic peridotites. Geochem Geophys Geosyst 8: Q02012. https://doi.org/10.1029/2006GC001373

Arai S., Takada S., Michibayashi K. and Kida M., 2004. Petrology of Peridotite Xenoliths from Iraya Volcano, Philippines, and its implication for dynamic mantle-wedge processes, J. Petrol., 45: 369-389, https://doi.org/10.1093/petrology/egg100

Auzende J.-M., Van de Beuque S., Régnier M., Lafoy Y. and Symonds P., 2000. Origin of the New Caledonian ophiolites based on a French-Australian seismic transect. Marine Geol., 162: 225-236. https://doi.org/10.1016/S0025-3227(99)00082-1

Avias J., 1967. Overthrust structure of the main ultrabasic New Caledonian massives. Tectonophysics, 4: 531-541. https://doi.org/10.1016/0040-1951(67)90017-0

Bach W. and Klein F., 2009. The petrology of seafloor rodingites: insights from geochemical reaction path modelling. Lithos, 112: 103-117. https://doi.org/10.1016/j.litho s.2008.10.022

Baghat S.S. and Marshak S., 1990. Microlithon alteration associated with development of solution cleavage in argillaceous limestone: textural, trace-elemental and stable-isotopic observations. J. Struct. Geol, 12:165-175. https://doi.org/10.1016/0191-8141(90)90002-G

Bai, W., Zhou, M. F. and Robinson, P. T., 1993. Possible diamond-bearing mantle peridotites and podiform chromitites in the Luobusa and Donqiao ophiolites, Tibet. Can. J. Earth Sci., 30: 1650-1659. https://doi.org/10.1139/e93-143

Barnes I., O'Neil J. and Trescases J., 1978. Present-day serpentinization in New Caledonia, Oman and Yugoslavia. Geochim. Cosmochim. Acta, 42: 144-145. https://doi.org/10.1016/0016-7037(78)90225-9

Beach A., 1974. A geochemical investigation of pressure solution and the formation of veins in a deformed greywacke. Contrib. Miner. Petrol., 46: 61-68. https://doi.org/10.1007/BF00377993

Beach A., 1977. Vein arrays, hydraulic fractures and pressure-solution structures in a deformed flysch sequence S.W. England. Tectonophysics, 40: 201-225. https://doi.org/10.1016/0040-1951(77)90066-X

Beccaluva L., Coltorti M., Giunta G., and Siena F., 2004. Tethyan vs. Cordilleran ophiolites: a reappraisal of distinctive tectono-magmatic features of supra-subduction complexes in relation to the subduction mode. Tectonophysics, 393: 163-174. https://doi.org/10.1016/j.tecto.2004.07.034

Bitoun G. and Récy J., 1982. Origine et évolution du bassin des Loyauté et de ses bordures après la mise en place de la série ophiolitique de Nouvelle-Calédonie: Contribution à l'étude géodynamique du sud-ouest Pacifique: Travaux et documents ORSTOM, Paris. 505-539.

Bizimis M., Salters V.J.M. and Bonatti E., 2000. Trace and REE content of clinopyroxenes from supra-subduction zone peridotites. Implications for melting and enrichment processes in island arcs. Chem. Geol., 165: 67-85. https://doi.org/10.1016/S0009-2541(99)00164-3

Bodinier J.-L. and Godard M., 2013. Orogenic, ophiolitic, and abyssal peridotites, in The Mantle and Core: Treatise on Geochemistry, 2nd ed., edited by K. K. Turekian and H. D. Holland, Elsevier, Oxford, U. K. https://doi.org/10.1016/B0-08-043751-6/02004-1

Bons P. and Jessell M., 1997. Experimental simulation of the formation of fibrous veins by localised dissolution-precipitation creep. Mineral. Mag., 61: 53-63 https://doi.org/10.1180/minmag.1997.061.404.06

Brongniart A., 1813. Essai de classification minéralogique des roches mélangées, Journal des Mines, XXXIV: 190-199.

Cai P., Lian D., Aitchison J.C., Cluzel D., Zhou R., Rui H., Boa R., Ma H., Yang J. and Masoud A.E., 2025. Geochemical constraints on subduction-related mantle metasomatism of the Tiébaghi ophiolitic lherzolite in New Caledonia. Lithos, 496-497: 107948. https://doi.org/10.1016/j.lithos.2025.107948

Caruso L. J. and Chernosky J. V., 1979. The stability of lizardite. Can. Mineral., 17: 757-769.

Chen C.F., Dai W., Wang Z.C., Liu Y.S., Li M., Becke H. and Foley, S.F., 2019. Calcium isotope fractionation during magmatic processes in the upper mantle. Geochim. Cosmochim. Acta, 249: 121-137. https://doi.org/10.1016/j.gca.2019.01.031

Chen C.F., Liu Y.S. Feng, L.P. Foley S.F., Zhou L., Ducea M.N. and Hu Z.C., 2018. Calcium isotope evidence for subduction-enriched lithospheric mantle under the northern North China Craton. Geochim. Cosmochim. Acta, 238: 55-67. https://doi.org/10.1016/j.gca.2018.06.038

Cluzel D., Aitchison J., Secchiari A., Montanini A., and Bosch D., 2020. New Caledonia Ophiolite, marginal rifting to fore-arc evolution. Acta Geologica Sinica (English Edition), 94 (supp.1): 9-10. https://doi.org/10.1111/1755-6724.14431

Cluzel D., Iseppi M. and Chen Y., 2021. Eocene pre- and syn-obduction tectonics in New Caledonia (Southwest Pacific). A case for oblique subduction, transcurrent tectonics and oroclinal bending; structural and paleomagnetic evidence. Tectonophysics, 811: 228875 https://doi.org/10.1016/j.tecto.2021.228875

Cluzel D., Aitchison J.C., Zhou R., Ireland T., Heizler M., Patias D., Lesimple S., Maurizot P., and Teyssier C., 2022. Direct dating of podiform chromitite: U-Pb (zircon, rutile) and $^{40}Ar/^{39}Ar$ (pargasite) evidence from Tiebaghi Cr deposit (New Caledonia). Ore Geol. Rev., 145: 104873. https://doi.org/10.1016/j.oregeorev.2022.104873

Cluzel D., Boulvais Ph., Iseppi M., Lahondère D., Lesimple S., Maurizot P., Paquette J.L., Tarantola A. and Ulrich M., 2019. Slab-derived origin of tremolite-antigorite veins in a supra-subduction ophiolite; the Peridotite Nappe (New Caledonia) as a case study. Int. J. Earth Sci., 109: 171-196. https://doi.org/10.1007/s0051-019-01796-6

Cluzel D., Jourdan F. Meffre S., Maurizot P., and Lesimple S., 2012. The metamorphic sole of New Caledonia ophiolite; $^{40}Ar/^{39}Ar$, U-Pb, and geochemical evidence for subduction inception at a spreading ridge. Tectonics, 31 https://doi.org/10.1029/2011TC003085

Cluzel D., Meffre S., Maurizot P.and Crawford A.J., 2006. Earliest Eocene (53 Ma) convergence in the Southwest Pacific; evidence from pre-obduction dikes in the ophiolite of New Caledonia. Terra Nova., 18: 395-402. https://doi.org/10.1111/J.1365-3121.2006.00704.X

Cluzel D., Montanini A., Secchiari A., Ferrari E., Heizler M., Jourdan F., Meffre S., Zhou R. and Teyssier C., 2024. New geochemical and age ($^{40}Ar/^{39}Ar$ and U-Pb) constraints on forearc intrusive rocks from New Caledonia Ophiolite; diversity of melts generated at hot (transcurrent) subduction inception. J. Geol. Soc., 181: 1: jgs2023-145. https://doi.org/10.1144/jgs2023-145

Cluzel D., Pattier F., Zhou R., Meffre S., Aitchison J.C., Maurizot P., Mathian M. and Devidal J.L., 2025. Provenance reassessment of Eocene turbidites, New Caledonia: Inferences for obduction models. Geochem. Geophys. Geosys., 26: e2025GC012430. https://doi.org/10.1029/2025GC012430

Cluzel D., Ulrich M., Jourdan F., Paquette J.L., Audet M.A., Secchiari A. and Maurizot P., 2016. Early Eocene clinoenstatite boninite and boninite-series dikes of the ophiolite of New Caledonia; a witness of slab-melt enrichment of the mantle wedge in a nascent volcanic arc. Lithos, 260: 429-442. https://doi.org/10.1016/j.lithos.2016.04.031

Cluzel D., Whitten M., Meffre S., Aitchison J.C. and Maurizot P., 2017. A reappraisal of the Poya Terrane (New Caledonia). Accreted Late Cretaceous marginal basin upper crust, passive margin sediments and Eocene E-MORB sill complex. Tectonics, 37: 48-70. https://doi.org/10.1002/2017TC004579

Cluzel D., Aitchison J. C. and Picard C., 2001. Tectonic accretion and underplating of mafic terranes in the Late Eocene intra-oceanic fore-arc of New Caledonia (Southwest Pacific): geodynamic implications. Tectonophysics, 340: 23-60. https://doi.org/10.1016/S0040-1951(01)00148-2

Collot J.-Y. and Missègue F., 1986. Extension de la formation des basaltes de la côte ouest et de la zone d'enracinement des péridotites dans le Grand Lagon Nord de la Nouvelle-Calédonie: données géophysiques. Compt. Rend. Acad. Sci., 303, Série 2, 16: 1437-1442.

Collot J.-Y., Rigolot P. and Missegue F., 1988. Geologic structure of the northern New Caledonia Ridge, as inferred from magnetic and gravity anomalies. Tectonics, 7: 991-1013. https://doi.org/10.1029/TC007i005p00991

Corre M., Brunet F., Schwartz S., Gautheron C., Agranier A. and Lesimple S., 2023. Quaternary low-temperature serpentinization and carbonation in the New Caledonia ophiolite. Sci. Rep., 13: 19413. https://doi.org/10.1038/s41598-023-46691-y

Coudray J., 1976. Recherches sur le Néogène et le Quaternaire marin de la Nouvelle Calédonie. Contribution de l'étude sédimentologique à la connaissance de l'histoire géologique post-éocène (Fondation Singer-Polignac edition). Expéditions françaises sur les récifs coralliens de la Nouvelle-Calédonie, 8.

Crawford A.J., Faloon T.J. and Green D.H., 1989. Classification, petrogenesis and tectonic setting of boninites. In: Crawford A.J. (Ed.). Boninites and related rocks. Unwin Hyman, London, 2-49. ISBN. 978-0044450030.

Deville E. and Prinzhofer A., 2016. The origin of N2-H2-CH4-rich natural gas seepages in ophiolitic context: A major and noble gases study of fluid seepages in New Caledonia. Chem. Geol., 440: 139-147. https://doi.org/10.1016/j.chemgeo.2016.06.011

Dilek Y., 2003. Ophiolite concept and its evolution, in: Dilek Y. and Newcomb S. (Eds.). Ophiolite concept and the evolution of geological thought: Boulder, Colorado, Geol. Soc. Amer. Spec. Paper, 373: 1-16. http://dx.doi.org/10.1130/0-8137-2373-6.1

Dilek Y., and Furnes H., 2014. Ophiolites and Their Origins. Elements, 10: 93-100. https://doi.org/10.2113/gselements.10.2.93

DIMENC-SGNC-BRGM, 2010. Online geological map of New Caledonia. Government of New Caledonia. https://georep.nc

Durney D.W., 1972. Solution-transfer, an important geological deformation mechanism. Nature, 235: 315-317. https://doi.org/10.1038/235315a0DO

Durney D.W., 1976. Pressure-solution and crystallization deformation. Phil. Trans. R. Soc. London Ser. A Math Phys Sci, 283: 229-240.

Elderfield H., 1986. Strontium isotope stratigraphy. Palaeogeography, Palaeoclimatology, Palaeoecology, 57: 71-90. https://doi.org/10.1016/0031-0182(86)90007-6.

Evensen N.M., Hamilton P.J. and O'Nions R.K., 1978. Rare earth abundance in chondritic meteorites. Geochim. Cosmochim. Acta, 42: 1199-1212. https://doi.org/10.1016/0016-7037(78)90114-X

Fantle M.S., and Tipper E.T., 2014a. Calcium isotopes in the global biogeochemical Ca cycle: implications for development of a Ca isotope proxy. Earth Sci. Rev. 129, 148-177. https://doi.org/10.1016/j.earscirev.2013.10.004

Fantle M.S., and Tipper E.T., 2014b. Corrigendum to Calcium isotopes in the global biogeochemical Ca cycle: implications for development of a Ca isotope proxy (Earth-Science Reviews, 129, 148-177). Earth-Science Reviews 131, 149 https://doi.org/10.1016/j.earscirev.2014.02.002

Ferrari E., 2022. Mantle heterogeneities in rifting-related and supra-subduction settings: examples from External Ligurian and New Caledonia ophiolites. PhD Thesis, University of Parma, Italy.

Frost B.R., Evans K.A., Swapp S.M., Beard J.S. and Mothersole F.E., 2013. The process of serpentinization in dunite from New Caledonia. Lithos, 178: 24-39. https://doi.org/10.1016/j.lithos.213.02.002

Fu, B., Bröcker M., Ireland T., Holden P. and Kinsley L.P.J., 2015. Zircon U-Pb, O, and Hf isotopic constraints on Mesozoic magmatism in the Cyclades, Aegean Sea, Greece. International J. Earth Sci., 104: 75-87. https://doi.org/10.1007/s00531-014-1064-z.

Furnes H., and Dilek, Y., 2017. Geochemical characterization and petrogenesis of intermediate to silicic rocks in ophiolites: A global synthesis. Earth-Sci. Rev., 166, 1-37. http://dx.doi.org/10.1016/j.earscirev.2017.01.001

Gautier P., Quesnel B., Boulvais P. and Cathelineau M. 2016. The emplacement of the Peridotite Nappe of New Caledonia and its bearing on the tectonics of obduction. Tectonics, 35: 3070-3094. https://doi.org/10.1002/2016TC004318

Griffin W.L., Afonso J.C., Belousova E.A., Gain S.E., Gong X.H., Gonzalez-Jimenez J.M., Howell D., Huang J.X., McGowan N., Pearson N.J., Satsukawa T., Shi R., Williams P., XiongQ., Yang, J.S., Zhang M. and O'Reilly S.Y., 2016. Mantle Recycling: Transition Zone Metamorphism of Tibetan Ophiolitic Peridotites and its Tectonic Implications. J. Petrol., 57: 655-684. https://doi.org/10.1093/petrology/egw011

Harlow G.E., and Sorensen S.S., 2005. Jade (nephrite and jadeitite) and serpentinite: metasomatic connections. Int. Geol. Rev., 47: 113-146. https://doi.org/10.2747/0020-6814.47.2.113

Hemming S.R., van de Flierdt T., Goldstein S L., Franzese A.M., Roy M., Gastineau and G., Landrot G., 2007. Strontium isotope tracing of terrigenous sediment dispersal in the Antarctic Circumpolar Current: Implications for constraining frontal positions. Geochem. Geophys. Geosys., 8, 6. https://doi.org/10.1029/2006GC001441

Henderson P. (1984) Rare Earth Element Geochemistry. Elsevier Science Publishers B.V., Amsterdam, 510 p. ISBN: 978-0-444-42148-7

Herzberg C., 2004.Geodynamic Information in Peridotite Petrology. J. Petrol., 45: 2507-2530. https://doi.org/10.1093/petrology/egh039

Ishimaru S., Arai S., Ishida Y., Shirasaka M. and Okrugin V.M., 2007. Melting and multi-stage metasomatism in the mantle wedge beneath a frontal arc inferred from highly depleted peridotite xenoliths from the Avacha Volcano, Southern Kamchatka, J. Petrol.. 48: 395-433. https://doi.org/10.1093/petrology/egl065

Jean M.M. and Shervais J.W., 2017. The distribution of fluid mobile and other incompatible trace elements in orthopyroxene from mantle wedge peridotites. Chem. Geol. 457 118-130. https://doi.org/10.1016/j.chemgeo.2017.03.017

Kamenetsky V., Sobolev A.V., Eggins S.M.; Crawford, A.J., and Arculus, R.J., 2002. Olivine-enriched melt inclusions in chromites from a low-Ca boninites, Cape Vogel, Papua New Guinea: evidence for ultramafic primary magma, refractory mantle source and enriched components. Chem. Geol. , 183, 1-4: 287-303. https://doi.org/10.1016/S0009-2541(01)00380-1

Kapsiotis A., Ewing Rassios A., Antonelou A. and Tzamos E., 2016. Genesis and multi-episodic alteration of zircon-bearing chromitites from the Ayios Stefanos Mine, Othris massif, Greece: assessment of an unconventional hypothesis on the origin of zircon in ophiolitic chromitites. Minerals, 6: 124. https://doi.org/10.3390/min6040124

Kelemen P.B., 1990. Reaction Between Ultramafic Rock and Fractionating Basaltic Magma I. Phase Relations, the Origin of Calc-alkaline Magma Series, and the Formation of Discordant Dunite. J. Petrol., 31: 51-98. https://doi.org/10.1093/petrology/31.1.51

Kimura J.-I., Gill J.B., Kunikiyo T., Osaka I., Shimoshioiri Y., Katakuse M., Kakubuchi S., Nagao T., Furuyama K., Kamei A., Kawabata H., Nakajima J., van Keken P.E., and Stern R.J., 2014. Diverse magmatic effects of subducting a hot slab in SW Japan: Results from forward modeling, Geochem. Geophys. Geosyst., 15: 691-739, htps://doi.org/10.1002/2013GC005132

König S., Münker C., Schuth S., Luguet A.. Hoffmann E. and Kuduon J., 2010. Boninites as windows into trace element mobility in subduction zones. Geochim. Cosmochim. Acta74, 2: 684-704. https://doi.org/10.1016/j.gca.2009.10.011

Koutsovitis P., Magganas A., Pomonis P., and Ntaflos T., 2013. Subduction related rodingites from East Othris, Greece: mineral reactions and physicochemical conditions of formation. Lithos, 172-173:139-157. https://doi.org/10.1016/j.litho s.2013.04.009

Kurat G., Palme H., Embey-Isztin A., Touret J., Ntaflos T., Spettel B., Brandstätten F., Palme C., Dreibus G. and Prinz M., 1993. Petrology and geochemistry of peridotites and associated vein rocks of Zabargad Island, Red Sea, Egypt. Mineral. Petrol., 48: 309-341. https://doi.org/10.1007/BF01163106

Laborda-López C., Marchesi C., López Sánchez-Vizcaíno V., Gómez-Pugnaire M.T., Dale C.W., Jabaloy-Sánchez A., Padrón-Navarta J.A., Román-Alpiste M.J., and Garrido C.J., 2020. Geochemical evolution of rodingites during subduction: insights from Cerro del Almirez (southern Spain). Lithos, 370-371: 105639. https://doi.org/10.1016/j.lithos.2020.105639

Le Bayon B., Maurizot P., Reninger P. A., Lesimple S., Iseppi M., Alizert L., Perrin J. and Zhou R., 2023. Geometry and deformation of the sole of a large obducted ophiolitic unit: Insights from surface geology and airborne electromagnetics - Peridotite Nappe, New Caledonia. New Zealand J. Geol. Geophys., 68: 1-19. https://doi.org/10.1080/00288306.2023.2239187

Leblanc M. and Violette J.-F., 1983. Distribution of aluminum-rich and chromium-rich chromite pods in ophiolite peridotites. Econ, Geol. 78: 293-301. https://doi.org/10.2113/gsecongeo.78.2.293

Li H., Arculus R.J., Ishizuka O., Hickey-Vargas R., Yogodzinski G.M., McCarthy A., Kusano Y., Brandl P.A., Savov I.P., Tepley F.J. and Sun W., 2021. Basalt derived from highly refractory mantle sources during early Izu-Bonin-Mariana arc development. Nat. Comm., 12: 1723. https://doi.org/10.1038/s41467-021-21980-0.

Lian, D., Yang, J., Wiedenbeck, M., Dilek, Y., Rocholl, A. and Wu, W., 2018. Carbon and nitrogen isotope, and mineral inclusion studies on the diamonds from the Pozanti-Karsanti chromitite, Turkey. Contrib. Mineral. Petrol., 173: 1-18. https://doi.org/10.1007/s00410-018-1499-5

Lian, D.Y. Liu, F. Cai, P.J. Wu, W.W. Li, J. Majka, J. Xu, Z.Q. Yang, J.S. 2024. Osmium and zinc isotope constraints on the origin of chromitites from the Yarlung-Zangbo ophiolites, Tibet, China. Mineralium Deposita, 59, 1089-1107. https://doi.org/10.1007/s00126-024-01252-9

Liu C.Z., Xu Y.and Wu, F.Y. 2019. Limited recycling of crustal osmium in forearc mantle during slab dehydration. Acta Geologica Sinica - English Edition, 93: 17-17. https://doi.org/10.1111/1755-6724.14160.

Luyendyk B.P., 1995. Hypothesis for Cretaceous rifting of east Gondwana caused by subducted slab capture. Geology, 23: 373-376. https://doi.org/10.1130/00917613(1995)023<0373:HFCROE>2.3.CO;2

Marchesi C., Garrido C.J., Godard M., Belley F. and Ferré E., 2009. Migration and accumulation of ultra-depleted subduction related melts in the Massif du Sud ophiolite (New Caledonia). Chem. Geol., 266: 171-186. https://doi.org/10.1016/j.chemgeo.2009.06.004

Marocchi M., Hermann J., Tropper P., Bargossi G.M., and Mair V., 2010. Amphibole and phlogopite in "hybrid" metasomatic bands monitor trace element transfer at the interface between felsic and ultramafic rocks (Eastern Alps, Italy). Lithos, 117:135-148. https://doi.org/10.1016/j.lithos.2010.02.011

Maurizot P. and Lesimple S., 2012. Le jade de Nouvelle-Calédonie. Aspects géologiques, gemmologiques et archéologiques. Geol. Survey of New Caledonia int. rep.

Maurizot P. and Cluzel D., 2014. Pre-obduction records of Eocene foreland basins in central New Caledonia (Southwest Pacific); an appraisal from surface geology and Cadart 1 borehole data. New Zealand J. Geol. Geophys., 57: 307-311. https://doi.org/10.1080/00288306.2014.885065

Maurizot P., Cluzel D., Meffre S., Campbell H. J., Collot J. and Sevin B. 2020a. Pre-Late Cretaceous basement terranes of the Gondwana active margin of New Caledonia. In: Maurizot P., and Mortimer, N. (Eds.). New Caledonia: Geology, Geodynamic Evolution and Mineral Resources. Geol. Soc.London, Mem., 51: 27-52. https://doi.org/10.1144/M51-2016-11

Maurizot P., Cluzel D., Patriat M., Collot J., Iseppi M., Lesimple S., Secchiari A., Bosch D., Montanini A., Macera P. and Davies H.L., 2020b. The Eocene Subduction-Obduction Complex of New Caledonia. In: Maurizot P., and Mortimer, N. (Eds.). New Caledonia: Geology, Geodynamic Evolution and Mineral Resources. Geol. Soc.London Mem., 51: 93-130. https://doi.org/10.1144/M51-2018-70

Maurizot P., Robineau B., Jeanpert J., Iseppi M., Lesimple S., Juillot F., Meyer,M., Fullenwarth P. and Mardhel V., 2023. Anatomy of an obducted ultramafic unit (Tiébaghi Massif - Peridotite Nappe -New Caledonia): Polyphase brittle tectonics constrained by fault-slip data and crack seal mineralogy. New Zealand J. Geol. Geophys., 68: 20-40. https://doi.org/10.1080/00288306.2023.2243851

McArthur J.M., Howarth R.J. and Shields G.A., 2012. Strontium Isotope Stratigraphy. In: Gradstein F., Ogg J. SchmitzM., Ogg G. The Geologic Time Scale 2012. Elsevier https://doi.org/10.1016/B978-0-444-59425-9.00007-X

McGowan N.M., Griffin W.L., González-Jiménez J.M., Belousova E., Afonso J.C., Shi, R., McCammon C.A., Pearson N.J. and O'Reilly S.Y., 2015. Tibetan chromitites: Excavating the slab graveyard. Geology, 43: 179-182. https://doi.org/10.1130/G36245.1

McInnes B.I.A., Gregoire M., Binns R.A., Herzig P.M., and Hannington M.D., 2001. Hydrous metasomatism of oceanic sub-arc mantle, Lihir, Papua New Guinea: Petrology and geochemistry of fluid-metasomatised mantle wedge xenoliths. Earth Planet. Sci. Lett., 188: 169-183. https://doi.org/10.1016/S0012-821X(01)00306-5

McLennan S.M., Taylor S.R., McCulloch M.T.and Maynard J.B., 1990. Geochemical and Nd-Sr isotopic composition of deep-sea turbidites: Crustal evolution and plate tectonic associations. Geochim. Cosmochim. Acta, 54: 2015-2050. https://doi.org/10.1016/0016-7037(90)90269-Q

Meffre, S., 1995. The development of island-arc related ophiolites and sedimentary sequences in New Caledonia. PhD thesis, University of Sydney, Australia, 258 pp.

Moghadam, H.S., Li, Q.L., Stern, R.J., Griffin, W.L. and O'Reilly, S.Y., 2022. Zircon xenocrysts in Late Cretaceous magmatic rocks in the Kermanshah Ophiolite: link to Iran continental crust supports the subduction initiation model. Int. Geol. Rev., 64: 3248-3259. https://doi.org/10.1080/00206814.2022.2043193

Monnin C., Chavagnac V., Boulart C., Ménez B., Gérard M., Gérard E., Pisapia C., Quéméneur M., Erauso G., Postec A., Guentas-Dombrowski L., Payri C., and Pelletier B., 2014. Fluid chemistry of the low temperature hyperalkaline hydrothermal system of Prony Bay (New Caledonia). Biogeosciences, 11: 5687 5706. https://doi.org/10.5194/bg-11-5687-2014

Moores E.M., 1982. Origin and emplacement of ophiolites. Rev. Geophys., 4: 735-760. https://doi.org/10.1029/RG020i004p00735

Mortimer N., Campbell H.J. et al., 2017. Zealandia: Earth's hidden continent. GSA Today, 27: 3:27-35. https://doi.org/10.1130/GSATG321A.1

Mothersole F.E., Evans K., Frost B.R., 2017. Abyssal and hydrated mantle wedge serpentinized peridotites: a comparison of the 15°20'N fracture zone and New Caledonia serpentinites. Contrib. Mineral. Petrol., 172: 69. https://doi.org/10.1007/s00410-017-1381-x

Moutte J., 1982. Chromite deposits of the Tiebaghi ultramafic massif, New Caledonia. Econ. Geol., 77: 576. https://doi.org/10.2113/gsecongeo.77.3.576

Murthy V.R., and Beiser E., 1968. Strontium isotopes in ocean water and marine sediments. Geochim. Cosmochim. Acta, 32: 10: 1121-1126. https://doi.org/10.1016/0016-7037(68)90111-7

Nicolas A. and Dupuy C., 1984. Origin of ophiolitic and oceanic lherzolites. Tectonophysics, 110: 177-187. https://doi.org/10.1016/0040-1951(84)90259-2

Nicolas A. and Prinzhofer A., 1983. Cumulative or Residual Origin for the Transition Zone in Ophiolites: Structural Evidence. J. Petrol., 24: 188-206. https://doi.org/10.1093/petrology/24.2.188

Niu, Y., 1997. Mantle melting and melt extraction processes beneath ocean ridges: evidence from abyssal peridotites. J. Petrol., 38: 1047-1074. https://doi.org/10.1093/petroj/38.8.1047

O'Hanley D.S., Chernosky J.V. Jr., and Wicks F.J., 1989. The stability of lizardite and chrysotile. Can. Mineral., 27: 483-493.

Orloff, O., 1968. Etude géologique et géomorphologique des massifs d'ultrabasites compris entre Houailou et Canala (Nouvelle-Caledonie). Mem. University Montpellier (France), 6: 79-175.

Paris J.P., 1981. Géologie de la Nouvelle-Calédonie: Un essai de synthèse. Mémoire du Bureau de Recherche Géologique et Minière, 113: 279 pp. ISBN-10, 2715950179. ISBN-13, 978-2715950177.

Parkinson I.J., and Pearce J.A., 1998. Peridotites from the Izu-Bonin-Mariana Forearc (ODP Leg 125): Evidence for Mantle Melting and Melt-Mantle Interaction in a Supra-Subduction Zone Setting, J. Petrol., 39: 1577-1618. https://doi.org/10.1093/petroj/39.9.1577

Patias D., Zhou R.J., Aitchison J.C., Cluzel D., Ireland T.R., Lian D.Y. and Yang J.S., 2024. Beyond zircon fingerprinting: Zircon and TiO_2 polymorphs constrain genealogy and evolution of the New Caledonian ophiolite. Chem. Geol., 644. https://doi.org/10.1016/j.chemgeo.2023.121841

Patriat M., Collot J. et al., 2018. New Caledonia obducted Peridotite Nappe, offshore extent and implications for obduction and postobduction processes. Tectonics, 37: 1-20. https://doi.org/10.1002/2017TC004722

Pearce J. A., Lippard S. J., and Roberts S., 1984. Characteristics and tectonic significance of supra-subduction zone ophiolites. Geological Society, London, Special Publications, 16: 77-94. https://doi.org/10.1144/GSL.SP.1984.016.01.66

Pearce J.A., and Reagan, M.K., 2019. Identification, classification, and interpretation of boninites from Anthropocene to Eoarchean using Si-Mg-Ti systematics. Geosphere, 15: 1008-037. https://doi.org/10.1130/GES01661.1

Pirard C., Hermann J. and O'Neill H., 2013. Petrology and geochemistry of the crust-mantle boundary in a nascent arc, Massif du Sud, New Caledonia. J. Petrol., 54: 1759-1792. https://doi.org/10.1093/petrology/egt030

Pisapia C., Gérard E., Gérard M., Lecourt L., Lang S.Q., Pelletier B., Payri C.E., Monnin C., Guentas L., Postec A., Quéméneur M., Erauso G. and Ménez B., 2017. Mineralizing Filamentous Bacteria from the Prony Bay Hydrothermal Field Give New Insights into the Functioning of Serpentinization-Based Subseafloor Ecosystems. Front. Microbiol., 8: 57. https://doi.org/10.3389/fmicb.2017.00057

Pollard D.D. and Segall P., 1987. Chapter 8: Theoretical displacements and stresses near fractures in rock: with applications to faults, joints, dikes, and solution surfaces. In: Atkinson B (Ed.). Fracture mechanics of rock. Academic Press, London, 277-349. https://doi.org/10.1016/C2009-0-21691-6

Pontoise B., Collot J.Y., Missegue F. and Latham G., 1982. Sismique réfraction dans le bassin des Loyauté: Résultats et discussion, in Equipe de Géologie-Géophysique du Centre ORSTOM de Nouméa: Contribution à l'étude géodynamique du Sud-Ouest Pacifique. Travaux et Documents ORSTOM, 147: 541-548

Prinzhofer A., and Allègre C.J., 1985. Residual peridotites and the mechanisms of partial melting. Earth Planet Sci. Lett. 74:251-265. https://doi.org/10.1016/0012-821x(85)90025-1

Prinzhofer A. and Nicolas A., 1980. The Bogota peninsula, New Caledonia: a possible oceanic transform fault. J. Geol., 88: 387-398. https://doi.org/10.1086/628523

Prinzhofer A., Nicolas A., Cassard D., MoutteJ., Leblanc M., Paris J.P. and Rabinovitch M., 1980. Structures in the New Caledonia peridotites-gabbros: implications for oceanic mantle and crust. Tectonophysics, 69: 85-112. https://doi.org/10.1016/0040-1951(80)90128-6.

Proenza J.A., González-Jiménez J.M., Garcia-Casco A., Belousova E., Griffin W.L., Talavera C., Rojas-Agramonte Y., Aiglsperger T., Navarro-Ciurana D. and Pujol-Solà N., 2018. Cold plumes trigger contamination of oceanic mantle wedges with continental crust-derived sediments: Evidence from chromitite zircon grains of eastern Cuban ophiolites. Geosci. Front., , 9: 1921-1936. https://doi.org/10.1016/j.gsf.2017.12.005

Python M., Yoshikawa M., Shibata T. and Arai S., 2011. Diopsidites and rodingites: serpentinization and Ca-metasomatism in the Oman Ophiolite Mantle. In: Dike swarms: keys for geodynamic interpretation. Springer, Berlin. https://doi.org/10.1007/978-3-642-12496-9_23

Quesnel B., Boulvais P., Gautier P., Cathelineau M., John C.M., Dierick M., Agrinier P. and Drouillet M., 2016. Paired stable isotopes (O, C) and clumped isotope thermometry of magnesite and silica veins in the New Caledonia Peridotite Nappe. Geochim. Cosmochim. Acta, 183: 234-249. https://doi.org/10.1016/j.gca.2016.03.021

Quesnel, B., Boulvais, P., Gautier, P., Cathelineau, M., Maurizot, P., Cluzel, D., Ulrich, M., Guillot, S., Lesimple, S., Couteau, C., 2013. Syn-tectonic, meteoric water-derived carbonation of the New Caledonia peridotite nappe. Geology 41, 1063 1066. https://doi.org/10.1130/g34531.1

Quesnel, B., Gautier, P., Cathelineau, M., Boulvais, P., Couteau, C., Drouillet, M., 2016b. The internal deformation of the Peridotite Nappe of New Caledonia: A structural study of serpentine-bearing faults and shear zones in the Koniambo Massif. J Struct Geol 85, 51 67. https://doi.org/10.1016/j.jsg.2016.02.006

Raia N.H., Whitney D.L., Teyssier C. and Lesimple S., 2022. Serpentinites of different tectonic origin in an exhumed subduction complex (New Caledonia, SW Pacific). Geochem., Geophys., Geosystems, 23. https://doi.org/10.1029/2022gc010395

Rodgers K.A., 1975. A Comparison of the Geology of the Papuan and New Caledonian Ultramafic Belts. J. Geol., 83: 47-60. https://doi.org/10.1086/628044

Rojas-Agramonte Y., Garcia-Casco A., Kemp A., Kröner A., Proenza J.A., Lázaro C. and Liu D., 2016. Recycling and transport of continental material through the mantle wedge above subduction zones: a Caribbean example. Earth Planet. Sci. Lett., 436: 93-107. https://doi.org/10.1016/j.epsl.2015.11.040

Rutter E.H., 1983. Pressure solution in nature, theory and experiment. J. Geol. Soc., 140: 725-740. https://doi.org/10.1144/gsjgs.140.5.0725

Sameshima T., Paris J.P., Black P.M. and Heming R.F., 1983. Clinoenstatite-bearing lava from Népoui, New Caledonia. Amer. Mineral., 68: 1076-1082.

Schwartz S., Guillot S., Reynard B., Lafay R., Debret B., Nicollet C., Lanari P. and Auzende A.L., 2013. Pressure-temperature estimates of the lizardite/antigorite transition in high pressure serpentinites. Lithos, 178: 197-210. https://doi.org/10.1016/j.lithos.2012.11.023

Secchiari A., Montanini A., and Cluzel D., 2022a.Temperatures and cooling rates recorded by the New Caledonia ophiolite: implications for cooling mechanisms in young forearc sequences. Geochem. Geophys. Geosys., 23: e2021GC009859. https://doi.org/10.1029/2021GC009859.

Secchiari A., Montanini A. and Cluzel D., 2022b. Hydrous mafic-ultramafic intrusives at the roots of a proto-arc: implications for crust building and mantle source heterogeneity in young fore arc regions. Contrib. Miner. Petrol., 177: 50. https://doi.org/10.1007/s00410-022-01912-x

Secchiari A., Montanini A., Bosch D., Macera P. and Cluzel D., 2016. Melt extraction and enrichment processes in the New Caledonia lherzolites: evidence from geochemical and Sr-Nd isotope data. Lithos, 260: 28-43. https://doi.org/10.1016/j.lithos.2016.04.030

Secchiari A., Montanini A., Bosch D., Macera P. and Cluzel D., 2018. The contrasting geochemical message from the New Caledonia gabbronorites: insights on depletion and contamination processes of the sub-arc mantle in a nascent arc setting. Contrib. Mineral. Petrol., 173: 66. https://doi.org/10.1007/s00410-018-1496-8

Secchiari A., Montanini A., Bosch D., Macera P. and Cluzel D., 2020a. Sr-Nd-Pb and trace element systematics of the New Caledonia harzburgites: tracking source depletion and contamination processes in a SSZ setting. Geosciences Frontiers, 11: 37-55. https://doi.org/10.1016/j.gsf.2019.04.004.

Secchiari A., Gleissner Ph., Li C., Goncharov A., Becker H., Bosch D. and Montanini A., 2020b. Highly siderophile and chalcophile element behaviour in abyssal-type and supra-subduction zone mantle: new insights from the New Caledonia ophiolite. Lithos, 354-355.https://doi.org/10.1016/j.lithos.2019.105338.

Secchiari A., Montanini A., Bosch D., Macera P., and Cluzel D., 2019. Origin of the spinel-pyroxene symplectites in the harzburgites from the New caledonia peridotite. Ofioliti, 44: 31-42. https://doi.org/10.4454/ofioliti.v44i1.463

Sevin B., Cluzel D., Maurizot P., Quesnel F., Ricordel-Prognon C. Chapronniere G, Folcher N. and Quesnel F. 2014. A drastic Lower Miocene regolith evolution triggered by post obduction slab break-off and uplift in New Caledonia. Tectonics, 33: 1787-1801. https://doi.org/10.1002/2014TC003588

Sevin B., Maurizot P., Cluzel D., Tournadour E., Etienne S., Folcher N., Jeanpert J., Collot J., Iseppi M. Meffre S. and Patriat M., 2020. Post obduction evolution of New Caledonia. In: Maurizot P., and Mortimer, N. (Ed.). New Caledonia: Geology, Geodynamic Evolution and Mineral Resources. Geol. Soc. London, Mem., 51: 147-188. https://doi.org/10.1144/M51-2018-74

Sevin B., Ricordel-Prognon C., Quesnel F., Cluzel D. and Maurizot P., 2012. First paleomagnetic dating of ferricrete in New

Caledonia: new insight on the morphogenesis and paleoweathering of 'Grande Terre'. Terra Nova ,24: 77-85. https://doi.org/10.1111/j.1365-3121.2011.01041.x

Shervais J. W., 2001. Birth, death, and resurrection: The life cycle of suprasubduction zone ophiolites. Geochem. Geophys. Geosyst. 2: 220925(8). https://doi.org/10.1029/2000GC000080

Shervais J.W. and Jean M.M., 2012. Inside the subduction factory: Modeling fluid mobile element enrichment in the mantle wedge above a subduction zone. Geochim. Cosmochim. Acta, 95: 270-285. http://dx.doi.org/10.1016/j.gca.2012.07.006

Shervais J., Reagan M., Godard M., Prytulak J., Ryan J., et al., 2021. Magmatic response to subduction initiation, Part II: boninites and related rocks of the Izu-Bonin arc from IOPD Expedition 352. Geochem. Geophys. Geosys., 22 (1). https://doi.org/10.1029/2020GC009093

Shor G.G., Kirk H.K. and Menard H.W., 1971. Crustal structure of the Melanesian area: J. Geophys. Res., 76: 2562-2586. https://doi.org/10.1029/JB076i011p02562

Sivell W.J. and Waterhouse J.B., 1986. The geochemistry, origin, and tectonic significance of rodingites from the Dun Mountain Ultramafics, D'Urville Island, New Zealand. New Zealand J. Geol. Geophys., 29: 9-27. https://doi.org/10.1080/00288306.1986.10427519

Stern R.J., 2004. Subduction initiation: spontaneous and induced. Earth Planet. Sci. Lett., 226: 275-292. https://doi.org/10.1016/j.epsl.2004.08.007

Titus S.J., Maes S.M., Benford B., Ferre E.C. and Tikoff B., 2011. Fabric development in the mantle section of a paleotransform fault and its effect on ophiolite obduction, New Caledonia. Lithosphere, 3: 221-244, https://doi.org/10.1130/l122.1

Ulrich M., Munoz M., Boulvais Ph., Cathelineau M., Cluzel D., Guillot S. and Picard C., 2020. Serpentinization of New Caledonia peridotites: from depth to (sub-)surface. Contrib. Mineral. Petrol., 175: 91. https://doi.org/10.1007/s00410-020-01713-0

Ulrich M., Muñoz M., Guillot S., Cathelineau M., Picard C., Quesnel B., Boulvais P. and Couteau, C., 2014. Dissolution-precipitation processes governing the carbonation and silicification of the serpentinite sole of the New Caledonia ophiolite. Contrib. Mineral. Petr., 167: 952. https://doi.org/10.1007/s00410-013-0952-8

Ulrich M., Picard C., Guillot S., Chauvel C., Cluzel D. and Meffre S. 2010. Multiple melting stages and refertilisation process as indicators for ridge to subduction formation: the New Caledonia Ophiolite. Lithos, 115: 223-236. https://doi.org/10.1016/j.lithos.2009.12.011

Van de Beuque S. 1999. Evolution géologique du domaine péri-Calédonien (sud-ouest Pacifique). PhD thesis Université de Bretagne Occidentale, Brest, France.

Veizer J., 1989. Strontium isotopes in seawater through time. Annual Rev. Earth Planet. Sci., 17: 141-167. https://doi.org/10.1146/annurev.earth.17.1.141

Vermeesch P., 2006. Tectonic discrimination diagrams revisited. Geochem. Geophys. Geosys., 7: Q06017. https://doi.org/10.1029/2005GC001092

Walker D.A., and Cameron W.E., 1983. Boninite primary magmas: Evidence from the Cape Vogel Peninsula, PNG. Contr. Mineral. and Petrol., 83: 150-158. https://doi.org/10.1007/BF00373088

Whattam S.A. and Stern R.J., 2011. The 'subduction initiation rule': a key for linking ophiolites, intra-oceanic forearcs, and subduction initiation. Contrib. Mineral. Petrol., 162: 1031-1045. https://doi.org/10.1007/s00410-011-0638-z

Wenner D.B. and Taylor H.P. Jr., 1974. D/H and O^{18}/O^{16} studies of serpentinization of ultramafic rocks, Geochim. Cosmochim. Acta, 38: 1255-1286, https://doi.org/10.1016/0016-7037(74)90120-3

Wood D.A., 1980. The application of a Th-Hf-Ta diagram to problems of tectonomagmatic classification and to establishing the nature of crustal contamination of basaltic lavas of the British Tertiary volcanic province. Earth Planet. Sci. Lett., 50: 11-30. https://doi.org/10.1016/0012-821X(80)90116-8

Wood B.J. and Turner S.P., 2009. Origin of primitive high-Mg andesite: Constraints from natural examples and experiments. Earth Planet. Sci. Lett., 283: 59-66. http://doi.org/10.1016/j.epsl.2009.03.032

Xiong F., Yang J., Robinson P.T., Dilek Y., Milushi I., Xu X., Zhou W., Zhang Z. and Rong H., 2017. Diamonds Discovered from High-Cr Podiform Chromitites of Bulqiza, Eastern Mirdita Ophiolite, Albania. Acta Geologica Sinica (English Edition), 91: 455-468. https://doi.org/10.1111/1755-6724.13111

Xu Y. and Liu C.-Z., 2026. Two origins of dunites in the New Caledonia ophiolites melt-rock reaction versus fractional crystallization. Ofioliti, 51:1-13. https://doi.org/10.4454/ofioliti.v51i1.579

Xu Y., Liu C.-Z., Lin W., Shi X.-F., 2022. Ancient depletion signals in lherzolites from forearc region: Constraints from Lu-Hf isotope compositions. Geosci. Front., 13: 101259. https://doi.org/10.1016/j.gsf.2021.101259

Xu Y., Liu C-Z and Lin W., 2020. Melt extraction and reaction in the forearc mantle: Constraints from trace elements and isotope geochemistry of ultra-refractory peridotites of the New Caledonia Peridotite Nappe. Lithos, 380-381: 105882. https://doi.org/10.1016/j.lithos.2020.105882

Xu Y., Liu C.Z., Shi X.F., Lin W. 2022. Petrogenesis of Eocene mafic and felsic magmas in the New Caledonia ophiolite: geochemistry and geochronology constraints. International Geol. Rev., 4 (15): 2186-2203. https://doi.org/10.1080/00206814.2021.1978111

Yamamoto S., Komiya T., Yamamoto H., Kaneko Y., Terabayashi M., Katayama I., Iizuka T., Maruyama S., Yang J.S., Kon Y. and Hirata T., 2013. Recycled crustal zircons from podiform chromitites in the Luobusa ophiolite, southern Tibet. Island Arc, 22: 89-103. https://doi.org/10.1111/iar.12011

Yang, J., Wu, W., Lian, D., and Rui, H., 2021. Peridotites, chromitites and diamonds in ophiolites. Nature Reviews Earth and Environment, 2: 198-212. https://doi.org/10.1038/s43017-020-00138-4.

Yang J. S., Robinson P. T. and Dilek Y., 2014. Diamonds in Ophiolites. Elements, 10: 127-130. https://doi.org/10.2113/gselements.10.2.127

Yu M., Dilek Y., Yumul G.P. Jr, Yan Y., Dimalanta C.B. and Huang C.Y., 2020. Slab-controlled elemental-isotopic enrichments during subduction initiation magmatism and variations in forearc chemostratigraphy. Earth Planet. Sci. Lett., 538: 116217. https://doi.org/10.1016/j.epsl.2020.116217

Zheng, Y.F., 1993. Calculation of oxygen isotope fractionation in hydroxyl-bearing silicates. Earth Planet. Sci. Lett., 121: 247-263. https://doi.org/10.1016/0012-821x(93)90243-3.

Received, May 2, 2026
Accepted, May 26, 2026